International Journal of Bifurcation and Chaos, Vol. 21, No. 12 (2011) 3417–3456

DOI: 10.1142/S0218127411030647

MULTIFRACTALS, GENERALIZED SCALE INVARIANCE AND COMPLEXITY IN GEOPHYSICS

DANIEL SCHERTZER
LEESU, École des Ponts ParisTech, Université Paris-Est, 6-8 Av. B. Pascal, 77455 Marne-la-Vallée Cedex 2, France
Daniel.Schertzer@enpc.fr

SHAUN LOVEJOY
Physics Department, McGill University, 3600, University St., Montreal, Que. H3A 2T8, Canada
lovejoy@physics.mcgill.ca

Received March 10, 2011; Revised May 6, 2011

The complexity of geophysics has been extremely stimulating for developing concepts and techniques to analyze, understand and simulate it. This is particularly true for multifractals and Generalized Scale Invariance. We review the fundamentals, introduced with the help of pedagogical examples, then their abstract generalization is considered. This includes the characterization of multifractals, cascade models, their universality classes, extremes, as well as the necessity to broadly generalize the notion of scale to deal with anisotropy, which is rather ubiquitous in geophysics.

Keywords: Multifractals; generalized scale invariance; scaling; geophysics.

1. Introduction

Geophysics, especially atmospheric dynamics over various scale ranges (i.e. from micro-turbulence to climate dynamics), has been an inspiring complex system for elaborating innovative concepts and techniques. For instance, everyone has in mind, the Lorenz's paper of 1963 [Lorenz, 1963] and the corresponding "butterfly effect" paradigm. However, there have been numerous contributions, which showed that the complexity of geophysical phenomena could be much more considerable and of a somewhat different nature. This includes a rather different approach to predictability by Lorenz himself [Lorenz, 1969], fractals [Mandelbrot, 1983], strange attractors [Nicolis & Nicolis, 1984], self-organized criticality [Bak *et al.*, 1987; Bak & Tang, 1989], and stochastic resonance [Nicolis, 1981; Benzi *et al.*, 1982; Nicolis, 1982; Benzi, 2010]. This paper is focused on the fundamentals of multifractals and generalized scale invariance, and shows that they are rather at the crossroads of the aforementioned concepts. This is illustrated with the help of examples to understand, analyze and simulate nonlinear phenomena in geophysics over wide ranges of scales.

In a very general manner, multifractals are space or space-time fields — the latter being often called processes — that have structures at all scales. They are, therefore, a broad generalization of the (geometrical) fractals. Indeed, the set indicator function of a fractal set is a field that has only two values (= 0 or 1), whereas multifractal fields generally have multiple values, which are very often continuous. The property to have structures at all scales is trivially scale invariant since it does not depend on the scale of observation. This shows

that a multifractal field can also be defined as being invariant for a given scale transform, which is therefore a symmetry for this field. One says that it is a scale invariant field or a scaling field for short. We will give a very general, precise definition of this invariance and the corresponding scale transform that could be either deterministic or stochastic (e.g. involves only equality in probability distribution or other statistical equivalences), isotropic or not.

Due to their definition, multifractals are therefore not only quite general, but also quite fundamental. Indeed, not only are symmetry principles the building blocks of physics and many other disciplines [e.g. Weyl, 1952; Zee, 1986], but scale symmetry is an element of the extended Galilean invariance. Unfortunately, attention in mechanics, especially in point mechanics, has been initially focused on the space shifts between two (Galilean) frameworks that differ only by a constant relative velocity or a given rotation that define the pure Galilean group. But with extended bodies, therefore continuous mechanics, it broadened to other transforms such as scale dilations. In particular, [Sedov, 1972] pointed out in the wake of the Π-theorem of Buckimgam [Buckingham, 1914, 1915; Sonin, 2004] the key role of the latter in fluid mechanics, including for many applications (e.g. to estimate the blast wave of a nuclear explosion). More recently, Speziale [1985] demonstrated their relevance in selecting and defining relevant subgrid models in turbulence. This has been widely used under the denomination of self-similarity, but with unnecessary limitations. Indeed, the main goal was to find a unique scale transform under which the nonlinear dynamical equations (in particular, the Navier–Stokes equations associated with others, such as the advection-dissipation equation). This was mainly achieved by adimensionalising these equations with the help of various so-called characteristic quantities, including characteristic space and time scales. Multifractals are, in fact, invariant for a multiple scale symmetry and therefore correspond once again to a broad generalization of properties that were previously perceived in a too restrictive framework. We indeed have to go from scale analysis, a seminal example being the quasi-geostrophic approximation derivation by Charney [1948], to scaling analysis [Schertzer *et al.*, 2011] that we will briefly discuss in Sec. 8.4.

A not-so-trivial consequence of this multiplicity of scale symmetries is that these fields could be understood as an infinite hierarchy of embedded fractals, e.g. those supporting singularities higher than a given order. This is the source of the terminology, but more importantly of a rather straightforward manner to understand intermittency: higher and higher levels of "activity" of the field are concentrated on smaller and smaller fractions of the space. This provides a rather straightforward way to quantify and analyze intermittency. This easiness is in sharp contrast with the mathematical nature of a multifractal field: it is a (mathematical) measure, which is furthermore multi-singular. The fact that it is a measure implies that it is not a pointwise field with a given value at any given point, but it only yields an average value over any given (small) neighborhood of this point or an integration of a suitable set of "test functions". The fact it is multisingular with respect to the Lebesgue measure, i.e. does not admit a density with respect to the latter, means that its estimated density at larger and larger resolution diverges with various power-laws exponents. These singularity orders are called singularities for short. This can be therefore seen as a very broad generalization of the singular Dirac's measure (often improperly called function), whose mass is concentrated on a pointwise "atom" and therefore can be understood as a divergence of its density that becomes infinite at this point, whose dimension is zero. For multifractals, theirs mass is distributed on the embedded fractal sets mentioned above.

As discussed below, these generalizations, as well as their necessity, step-by-step became patent with the help of cascade models in turbulence and strange attractors. These models were first rather crude (e.g. discrete in scales) and apparently simple, but yielded nontrivial behaviors which were step-by-step recognized as escaping from the original framework of analysis, i.e. fractal analysis. Their present refined offsprings (e.g. continuous in scales) are generic models providing multifractal fields and related data analysis techniques. These models and multifractals have been used in a wide range of scientific disciplines, from ecology to financial physics, including high energy physics, geophysics, astrophysics, etc. *A priori*, all domains of nonlinear science and complex science are concerned, but geophysics remains a preeminent domain of applications.

To cover various aspects of multifractals and generalized scale invariance, the paper is organized as follows:

- Section 2 introduces the key notions of singular measures with the help of the pedagogical example of the rainrate at various resolutions,
- Section 3 introduces the cascade models in a phenomenological manner and two pedagogical models,
- Section 4 introduces the general multifractal framework with the codimension and the scaling moment functions and their duality via the Legendre transform, as well as a comparison between multifractal formalisms,
- Section 5 goes a bit further in formalism by introducing cascade generators, characteristic functions and multifractal scale symmetry in a general, yet precise manner,
- Section 6 is devoted to the question of universality, in particular to drastically reduce the number of parameters characterizing a multifractal,
- Section 7 pursues, in a given way, this discussion to address the question of models that are continuous in scales,
- Section 8 suggests how to broadly generalize the previous results with the help of generalized scales and Lie cascades in the framework of Generalized Scale Invariance, as well as their application to differential systems.
- Section 9 is focused on the question of extremes, particularly on heavy tails that are easily generated by multifractals, the relationship with self-organized criticality and related multifractal transitions.

Although this is already a long paper, it does not cover all the aspects of multifractals in geophysics. For instance, the question of multifractal predictability [Schertzer & Lovejoy, 2004b] is not discussed, but only evoked, in spite of the fact that it corresponds to a broad generalization of the results of [Lorenz, 1969]. More generally, and for the same reason, although the concepts are illustrated with the help of geophysical examples, this paper does not pretend to review in an exhaustive manner their applications to geophysics.

2. Singularities Everywhere in Geophysics?

To better appreciate the underlying physico-mathematical nature of a multifractal, let us consider the precipitation intermittency with the help of common sense intuition: most of the time it does not rain, furthermore, when it does rain its intensity can be extremely variable. In spite of this intuition, an adequate mathematical framework had been elusive for a while and has been seriously elaborated only during the last twenty five years. Indeed, the variability of precipitation — which occurs over a wide range of (space and time) scales and intensities — is beyond the scope of classical geophysics. A well-known symptom of this basic problem is that the basic hydro-meteorological quantity, the rain rate r, has a strong scale dependency, since it depends on the duration on which it is measured. This is illustrated by Fig. 1(a) that displays (from top to bottom) the Nîmes time series of rainrates $r_\lambda(t)$ from an hour resolution ($\lambda = 365 \times 24$) down to a year resolution ($\lambda = 1$):

$$r_\lambda(t) = \frac{\lambda}{T} \sum_i 1_{[\tau_i, \tau_{i+1}[}(t) R([\tau_i, \tau_{i+1}[); \quad \tau_{i+1} - \tau_i = \frac{T}{\lambda} \tag{1}$$

where $R([\tau_i, \tau_{i+1}[)$ is the rain accumulation (i.e. the rain received) during the time interval $[\tau_i, \tau_{i+1}[$ and 1_A denotes the indicator function of any set A. The intensity scale strikingly decreases with the resolution, e.g. the maximum decreases from 35 to 0.1 mm/h, which gives some credence that the variability decreases with decreasing resolution. Nevertheless, as emphasized in [Ladoy *et al.*, 1993b] the variability still exists in the yearly resolution. The classical assumption is that the rain accumulation is a regular (mathematical) measure $dR(t)$ with respect to the (Lebesgue) volume measure dt, i.e. $dR(t)$ admits a pointwise density $r(t)$, defined almost everywhere:

$$dR(t) = r(t)dt. \tag{2}$$

This density $r(t)$ is called the rainrate and is considered as the basic quantity of interest in hydrometeorology. However, this assumption implies that $r(t)$ would correspond to a scale *independent* small scale limit of $r_\lambda(t)(\lambda \to \infty)$, which is in contradiction with the observed strong scale dependency of $r_\lambda(t)$. On the contrary, as discussed at length in [Schertzer *et al.*, 2010], as well as in Sec. 4.1, the assumption that $dR(t)$ is a (multiple) singular measure with respect to the Lebesgue measure implies that $r_\lambda(t)$ exhibits power-law singularities at larger and larger resolutions:

$$r_\lambda(t) \approx \lambda^\gamma. \tag{3}$$

Figure 1(b) displays these singularities for the rainrate $r_\lambda(t)$ displayed in Fig. 1(a), resolution by resolution. The intensity of these singularities γ's is

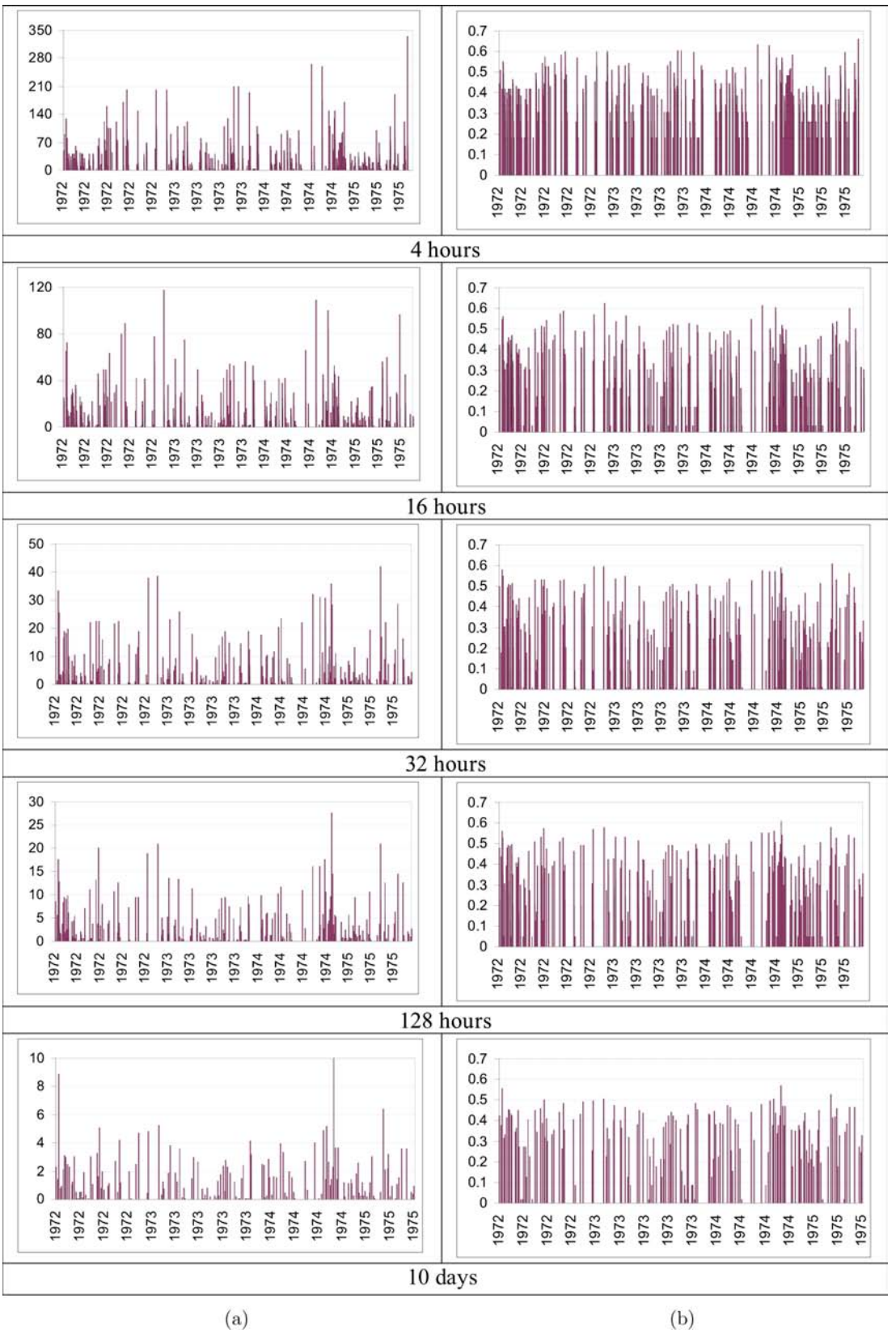

Fig. 1. Rainfall time series at Nîmes (1972–1975) from 1 h to 1 year duration: (a) the rainrate $r_\lambda(t)$ [Eq. (1)] exhibits a strong scale dependency, since its maximal value decreases from 35 to 0.1 mm/h from 1 h to 1 year duration (the unit of the intensity scale corresponds to 0.1 mm/h); (b) the corresponding singularities $\gamma \approx \log_\lambda(r_\lambda)$ show on the contrary a remarkable scale independency over the same range of durations. Reproduced from [Schertzer *et al.*, 2010].

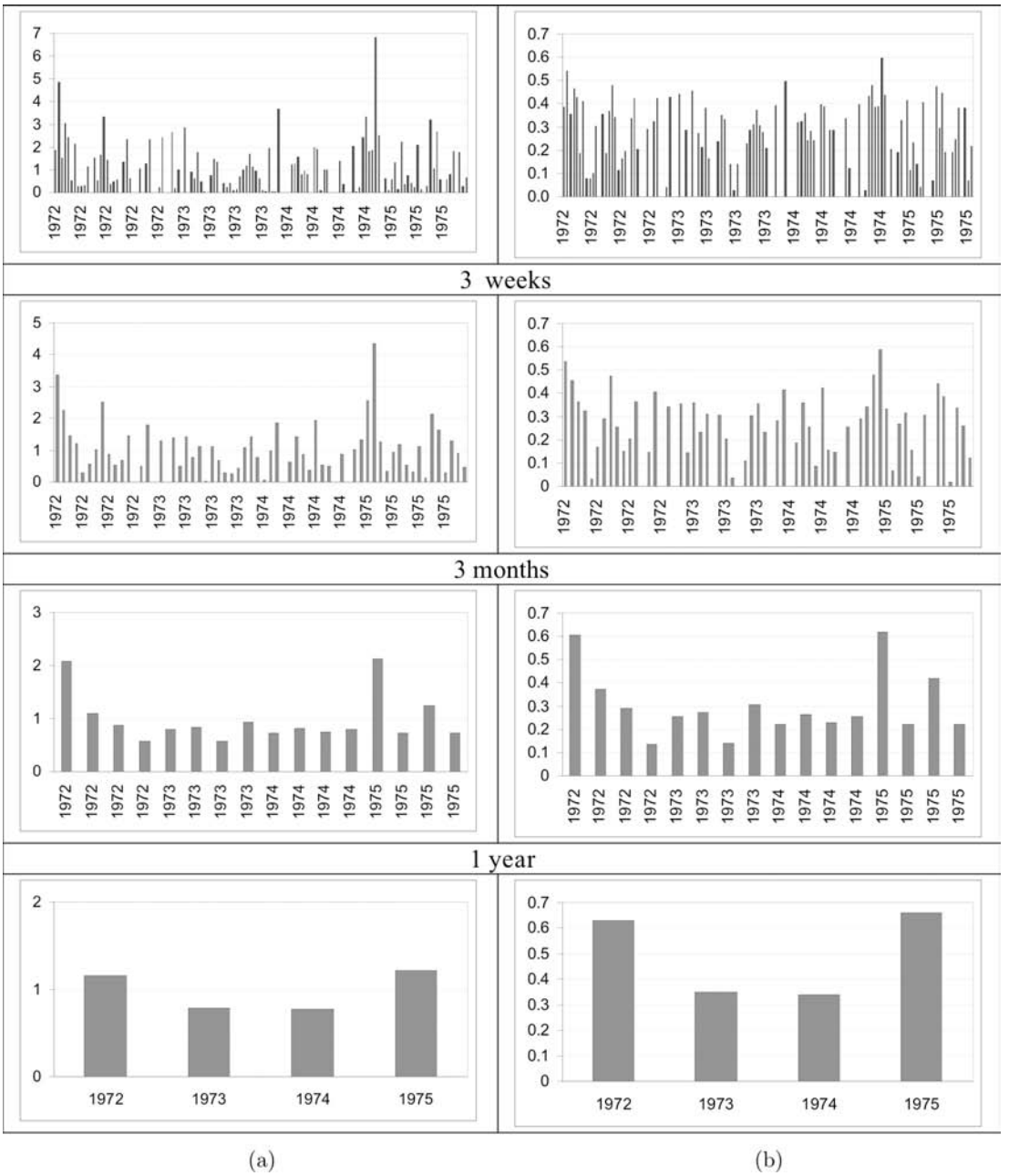

Fig. 1. (*Continued*)

strikingly independent of the scale, contrary to the rainrate intensity. One may also not note that there is not a unique value of γ, i.e. the measure $dR(t)$ is a multiple singular measure, with respect to the Lebesgue measure dt (which would yield $\gamma = 0$). Therefore — contrary to the usual hypothesis — there is no self-consistent definition of an instantaneous pointwise rain rate defined as a function $r(t)$.

We can proceed to a similar analysis with respect to space. This can be achieved with the help of statistical moments that should, as discussed in Sec. 4.2, display multiple power-laws generated by singularities. Figure 2 displays the statistical moments of the rain surrogate (radar reflectivity) over nearly four orders of magnitude in scale but could continue over another two orders of magnitude to smaller scales as observed with the help of ground radar data [Schertzer & Lovejoy, 1987].

We will show that the stochastic multifractal fields offer a very convenient and operational framework to handle such stochastic (multi-) singular measures. They indeed allow us to systematically characterize, model and understand extremely variable fields while avoiding the

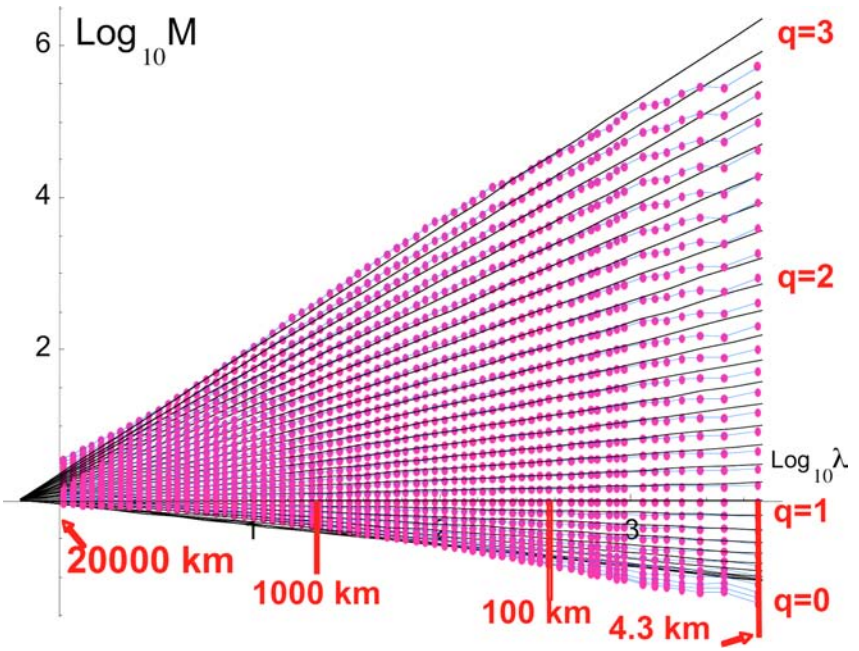

Fig. 2. Statistical moments $\langle r_\lambda^q \rangle$ of order q of statistical moments ($q = 0, 0.1, \ldots, 2.9$, bottom to top) with respect to their resolution λ in a log–log plot of the rainrate r_λ estimated by the radar of the TRMM satellite (≈ 1100 orbits) during a duration Δt and across a horizontal section $\Delta x \Delta y$ (x along the satellite path, y transverse to it), with $\Delta y = 4.3\,\mathrm{km}$, $\Delta x = L_{\mathrm{earth}}/\lambda$ ($L_{\mathrm{earth}} = 20\,000\,\mathrm{km}$). Straight lines correspond to power law fits. Reproduced from [Lovejoy *et al.*, 2008a].

restrictive homogeneity assumptions implicit in the conventional approaches. While traditional numerical approaches are forced to use drastic scale truncations, to transform partial differential equations (PDE's) into ordinary differential equations (ODE's), to make arbitrary regularity assumptions, and to perform *ad-hoc* and unjustified parameterizations (if only for the nonexplicit "subgrid" scales), these classical manipulations (and mutilations) violate a fundamental symmetry of nonlinear PDE's: their scale invariance (see Fig. 4). Even in spite of these (over) simplifying assumptions, the consequences of such choices are ultimately complex and unwieldy numerical codes. Often the relevance of such codes, is questionable and furthermore as their scales are quite different from those of observations, they are often only intercompared with other (similar) models. Multifractal analyses of these models are therefore rather indispensable to evaluate their

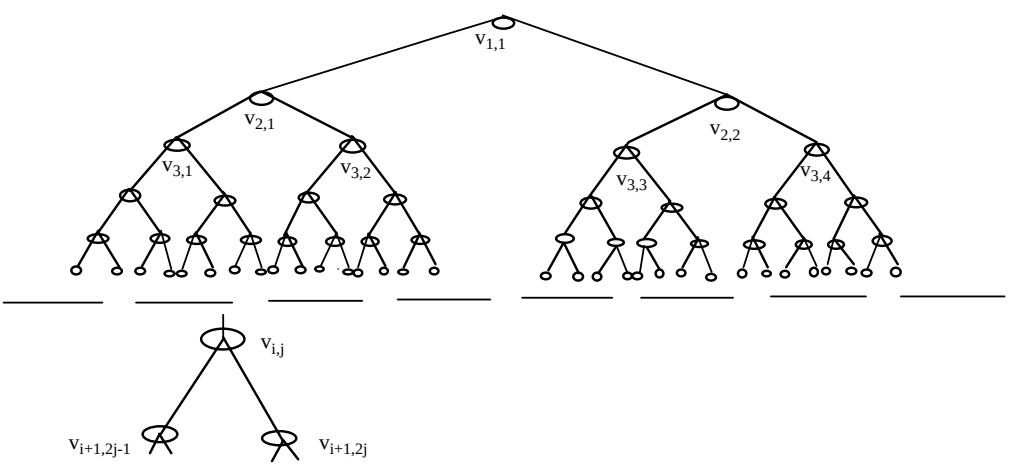

Fig. 3. A rather general scheme of a (deterministic) cascade process, which actually corresponds to a simplification of the Navier–Stokes equations, where only direct interactions between eddies and their offsprings are preserved. Reproduced from [Chigirinskaya & Schertzer, 1996].

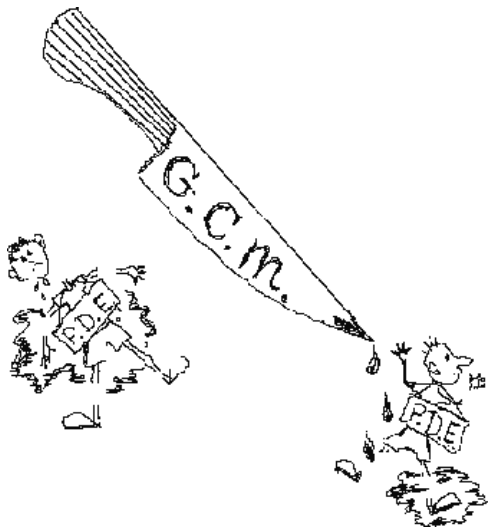

Fig. 4. A polemical illustration of the drastic reduction of Partial Differential Equations to Ordinary Differential Equations in General Circulation Models. Reproduced from [Schertzer & Lovejoy, 1993].

performance [Stolle *et al.*, 2009; Lovejoy & Schertzer, 2011; Gires *et al.*, 2011]. Furthermore, they could be as well indispensable to develop stochastic parametrizations, whose necessity is more and more recognized [Palmer & Williams, 2010], in order to reach the intrinsic predictability limits, which are themselve multifractal [Schertzer & Lovejoy, 2004a].

Concerning multifractal modeling, cascade models (see Fig. 3 for an illustration) are generic multifractal processes. Indeed, they are built up with the help of an elementary scale invariant process that is hierarchically repeated scale after scale along a hierarchical scaling tree of smaller and smaller structures. They therefore generate scaling fields and yield a rather straightforward way to understand that extreme variability over a very large range of scales may merely result from the repetition scale after scale of a given elementary process or interactions between neighboring scales.

This phenomenological idea can be traced back to Richardson's celebrated poem on self-similar cascades [Richardson, 1922] describing atmospheric dynamics as a cascade process. However, it required some time and various developments before providing well-defined models [Yaglom, 1966; Mandelbrot, 1974; Frisch *et al.*, 1978] and to become rigorously conceptualized with the help of fractals [Mandelbrot, 1977, 1983].

Then it evolved (after 1983), into a multifractal approach. The earliest scale invariant multifractal models, which we will review, are superficially quite simple phenomenological "toy models". Nevertheless, they yield exotic phenomena (exotic compared to conventional smooth mathematical descriptions of the real world...) and have highly nontrivial consequences. For example, as we will see later, simple cascade models already give rise to a fundamental difference between observables and truncated processes, and such a difference is a general property of the wide class of "hard" multifractal processes (which distinguish between "dressed" and "bare" properties respectively) as discussed in Sec. 9. These models produce hierarchies of self-organized random structures.

3. Phenomenology of Cascades

Starting with [Richardson, 1922], the phenomenology of (scalar) turbulent cascades was first discussed in the context of hydrodynamic turbulence where the structures are "eddies". Since we simply follow how the "activity", measured by the turbulent energy flux to smaller scales in turbulence, becomes more and more inhomogeneous as large structures break up into smaller and smaller scales, cascades are a very general paradigm.

The key assumption in phenomenological models of turbulence (which became explicit with the pioneering work of [Novikov & Stewart, 1964; Yaglom, 1966; Mandelbrot, 1974] is that successive steps (independently) define the fraction of the flux of energy distributed over smaller scales. It should be clear that the small scales cannot be regarded as adding energy; they only modulate the energy passed down from larger scales. The explicit hypothesis is that the fraction of the energy flux (more generally the "activity") from a parent structure to an offspring will be determined in a scale invariant manner.

In the (pedagogical) case of "discrete (in scale) cascade models" "eddies" are defined by the hierarchical and iterative division of a D-dimensional cube into smaller subcubes, with a constant ratio of scales λ_1 (greater than 1, very often equal to 2, see Fig. 3). More precisely, for each $n \in N$, the initial D-dimensional cube Δ_0^0 of size L is divided step by step into λ_1^n smaller disjoint subcubes $\Delta_n^{\underline{i}}$ ($i_j = 0, 1, \ldots (\lambda_1^n - 1); j = 1, 2, \ldots, D$) of size $\ell_n = L/\lambda_1^n$ that fully cover Δ_0^0. In other words, the λ_1-base coordinates of the corner $\underline{c}_{\underline{i}} = \underline{i}\lambda_1^{-n}$ of the subcube $\Delta_n^{\underline{i}}$ has only n digits. The density of the flux energy ε_n at the step n is taken to be strictly homogeneous

on each "subeddies" of scale ℓ_n, i.e. ε_n is a step function:

$$\varepsilon_n(\underline{x}) = \sum_{\underline{i}=\underline{0}}^{\underline{\lambda^n-1}} \varepsilon_n^{\underline{i}} 1_{\Delta_n^{\underline{i}}}(\underline{x}) \tag{4}$$

where $1_{\Delta_n^{\underline{i}}}$ is the indicator function of the subcube $\Delta_n^{\underline{i}}$. The energy density ε_{n-1} at step $n-1$ will be multiplicatively distributed to subeddies:

$$\varepsilon_n(\underline{x}) = \mu\varepsilon_n(\underline{x})\varepsilon_{n-1}(\underline{x}) \tag{5}$$

with the help of the following multiplicative increment decomposed on the same basis:

$$\mu\varepsilon_n(\underline{x}) = \sum_{\underline{i}=\underline{0}}^{\underline{\lambda^n-1}} \mu\varepsilon_n^{\underline{i}} 1_{\Delta_n^{\underline{i}}}(\underline{x}) \tag{6}$$

where the multiplicative increment components $\mu\varepsilon_n^{\underline{i}}$ are usually assumed to be identically and independently distributed (i.i.d.), as well as independent of the variables $\varepsilon_n^{\underline{i}}$, i.e. $\mu\varepsilon_n^{\underline{i}} \stackrel{d}{=} \mu\varepsilon$. Ensemble conservation, called "canonical conservation, of the flux corresponds to ($\langle\cdot\rangle$ denotes the ensemble average):

$$\langle\varepsilon_n\rangle = \langle\varepsilon_0\rangle \tag{7}$$

obviously it requires that the random variable $\mu\varepsilon$ defining the multiplicative increments should satisfy:

$$\langle\mu\varepsilon\rangle = 1. \tag{8}$$

This is also a sufficient condition, except if the cascade is degenerate, i.e. dies away after a finite number of steps ($\varepsilon_n \to 0$ almost surely). This arises when a too strong, unrealistic mean intermittency is chosen and we will see that this can be easily quantified.

In spite of their apparently simple yet somewhat awkward discretizations, these models are already able to give key insights into the fundamentals of cascade processes. This is confirmed using more realistic (continuous in scale) cascades, which are necessary to take into account other (statistical) symmetries (e.g. translation invariance, see Sec. 7).

3.1. *Unifractal insights and the simplest cascade model (β-model)*

The simplest cascade model, often called the β-model, takes the intermittency of turbulence into account by assuming [Novikov & Stewart, 1964; Mandelbrot, 1974; Frisch *et al.*, 1978] that eddies are either dead (inactive) or alive (active). This corresponds[1] to the fact that the random variable $\mu\varepsilon$, which defines the multiplicative increments, has only two states (see Fig. 5):

$$\begin{aligned} \Pr(\mu\varepsilon = \lambda_1^c) &= \lambda_1^{-c} \quad \text{(alive)} \\ \Pr(\mu\varepsilon = 0) &= 1 - \lambda_1^{-c} \quad \text{(dead)}. \end{aligned} \tag{9}$$

The boost $\mu\varepsilon = \lambda_1^c > 1$ is chosen so that the ensemble averaged ε is conserved [Eq. (8)]. At each step in the cascade, the fraction of the alive eddies

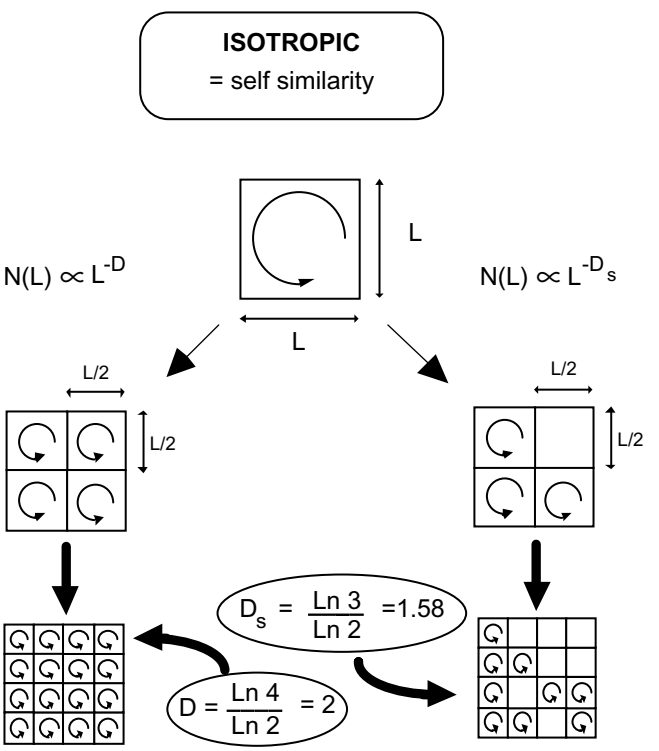

Fig. 5. A schematic of an isotropic discrete in scale cascade. The left-hand side shows a nonintermittent ("homogeneous") cascade, the right-hand side shows how intermittency can be modeled by assuming that not all sub-eddies are "alive". This is an implementation of the "β-model". From [Schertzer & Lovejoy, 1993].

[1]The β-model is often defined more vaguely than this. We follow the more precise stochastic presentation in [Schertzer & Lovejoy, 1984].

decreases by the factor $\beta = \lambda_1^{-c}$ (hence the name "β-model") and conversely their energy flux density is increased by the factor $1/\beta$ to assure (average) conservation. After n steps, this drastic and simple dichotomy is merely amplified by the total scale ratio λ_1^n:

$$\begin{aligned} \Pr(\varepsilon_n = \lambda_1^{nc}) &= \lambda_1^{-nc} \quad \text{(alive)} \\ \Pr(\varepsilon_n = 0) &= 1 - \lambda_1^{-nc} \quad \text{(dead)}. \end{aligned} \tag{10}$$

Hence either the density goes on to diverge with *an* (*algebraic*) *order of singularity* c, or is *at once* "killed" (set to zero)! Following the usual definition of a geometric codimension $C(A)$ of a set A of dimension $D(A)$ embedded in a space E of dimension $D(E)$:

$$C(A) = D(E) - D(A) \tag{11}$$

c is the codimension of the alive eddies and their corresponding (geometrical) dimension D_s is (if $c < D$):

$$D_s = D - c \tag{12}$$

which is often called the dimension of the support of turbulence. The degenerate case merely corresponds to $c \geq D$, i.e. when Eq. (10) would yield a negative dimension, which in fact corresponds to the fact that intermittency is so large that any activity almost surely vanishes after a finite number of steps.

3.2. *The simplest multifractal variant (the α-model)*

We already pointed out the mere occurrence/nonoccurence of rain is not too informative, e.g. in the Nimes time series [Fig. 1(a)] the daily average ≈ 2.1 mm mm/day is negligible compared to a 228 mm in a few hours — the October 1988 catastrophe in Nîmes! Furthermore, we already pointed out that this time series does not display a unique singularity [see Fig. 1(b) and the corresponding discussion in Sec. 2]. The variability of time series in Nimes is so significant that [Ladoy *et al.*, 1993a] and [Bendjoudi *et al.*, 1997] found evidence of divergence of high order statistical moments (a subject we will discuss more in Sec. 9). Similarly, Fig. 6 shows the qualitatively similar spatial distribution of the radar reflectivity of rain. This variability seems strikingly analogous to that of the energy flux cascade in turbulence (see schematic in Fig. 7), an analogy that turns out to be quite profound.

On the theoretical level the β-model turns out to be a poor approximation to turbulence because it is unstable under perturbation: as soon as one considers a more realistic alternative [Schertzer & Lovejoy, 1983] to the caricatural dead/alive dichotomy,

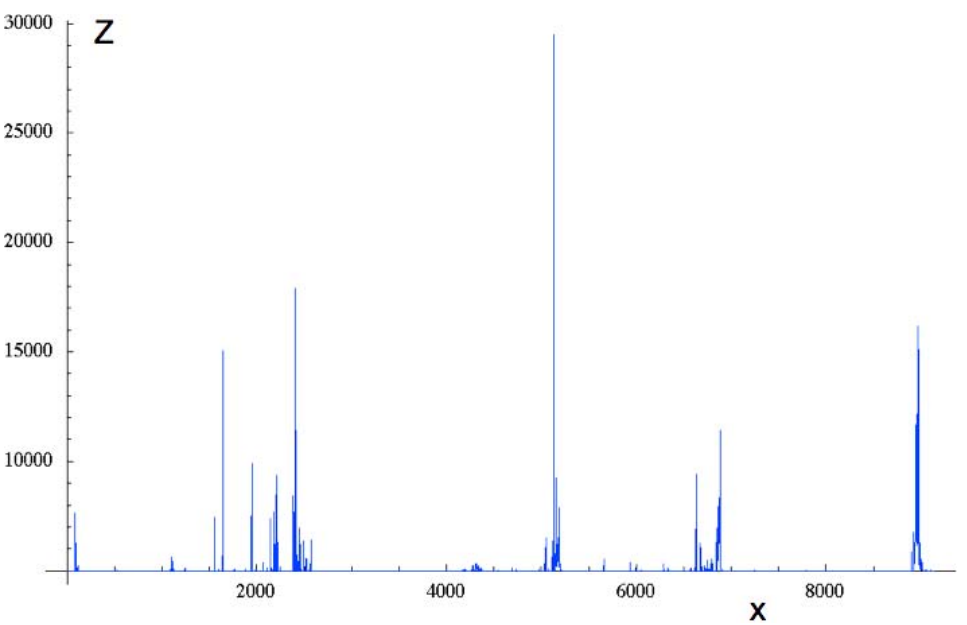

Fig. 6. A 1-D subsatellite section of satellite radar reflectivity (Z; units $\mathrm{mm}^6/\mathrm{m}^3$) of rain at a 4.3 km horizontal resolution, one full orbit showing flux-like spikes; the mean Z is $53\,\mathrm{mm}^6/\mathrm{m}^3$. From [Lovejoy *et al.*, 2008a].

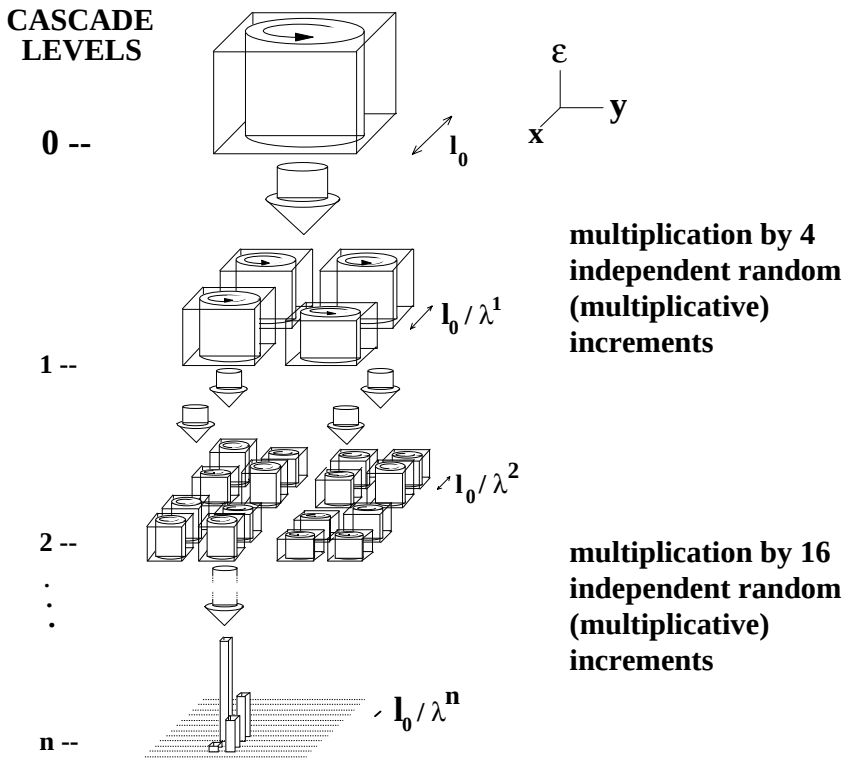

Fig. 7. A schematic of few steps of a discrete multiplicative cascade process, here the "α-model" with two "pure" singularities $\gamma_+ > 0$, $\gamma_- < 0$ (corresponding to the two values taken by the independent random increments $\lambda^{\gamma_+} > 1$, $\lambda^{\gamma_-} < 1$) leading to the appearance of mixed singularities γ ($\gamma_- \leq \gamma \leq \gamma_+$). From [Schertzer & Lovejoy, 1989b].

most of the peculiar properties of the β-model are lost. Indeed, let us consider the more realistic α-instability allowing subeddies to be either "more active" or "less active":

$$\begin{aligned} \Pr(\mu\varepsilon = \lambda_1^{\gamma_+}) &= \lambda_1^{c_+} \\ \Pr(\mu\varepsilon = \lambda_1^{\gamma_-}) &= 1 - \lambda_1^{c_+} = \lambda_1^{c_-} \end{aligned} \tag{13}$$

with $\gamma_+ > 0$, $\gamma_- < 0$. The β-model is recovered with $\gamma_+ = c = c_+; \gamma_- = -\infty$ and the "canonical" conservation [Eq. (7)] implies that there are really only two free parameters out of $c_+, c_-, \gamma_+, \gamma_-$, since it corresponds to:

$$\lambda^{\gamma_+ - c_+} + \lambda^{\gamma_- - c_-} = 1. \tag{14}$$

At step n, we have "mixed" singularities γ_r, $0 \leq r \leq 1$ resulting from linear combinations of the "pure" singularities $\gamma_0 = \gamma_-$, $\gamma_1 = \gamma_+$, where $r = n_+/n$ is the fraction of outcomes of γ_+ along the cascade branch leading to γ_r:

$$\begin{aligned} \gamma_r &= r\gamma_+ + (1-r)\gamma_- \\ \Pr(\varepsilon = (\lambda_1^n)^{\gamma_r}) &= \binom{n}{nr} (\lambda_1^n)^{rc_+ + (1-r)c_-} \simeq (\lambda_1^n)^{c(\gamma_r)} \\ c(\gamma_r) &= r(\mathrm{Log}_{\lambda_1}(r) + c_+) + (1-r)(\mathrm{Log}_{\lambda_1}(1-r) + c_-) \end{aligned} \tag{15}$$

where $\binom{n}{nr}$ is the number of nr-combinations of n objects and the Stirling formula is used to derive asymptotics for large n and for any given (and fixed) ratio $r = n_+/n$. The "p-model" [Meneveau & Sreenivasan, 1987] and the "binomial multifractal measure" correspond to microcanonical versions of the α-model, which means that the flux of energy is strictly conserved, not only on the ensemble average. This constraint fundamentally changes the properties of the processes, as we shall see below.

4. The General Multifractal Framework

4.1. *The codimension function $c(\gamma)$*

The pedagogical example of the α-model provides helpful insights into the general formalism necessary for more general cascade processes. For instance, in the α-model as the number of cascade steps n becomes large, one obtains asymptotic expressions [from Eq. (11)] which depend only on the total ratio of scale (denoted $\lambda = L/\ell \geq 1$):

$$\Pr(\varepsilon_\lambda \geq \lambda^\gamma \varepsilon_1) \sim \lambda^{-c(\gamma)} \tag{16}$$

This is a basic multifractal relation for multifractal processes, which merely states that the measure of the fraction of the probability space corresponding to the events

$$A_\lambda(\gamma) = \left\{(x,\omega) \in E \times \Omega \,|\, \varepsilon_\lambda(x,\omega) \geq \lambda^\gamma \varepsilon_1\right\} \quad (17)$$

has a (statistical) codimension $c(\gamma)$, the precise meaning of the asymptotic equivalence ($\lambda \to \infty$) denoted by $\sim$ will be discussed below. As already emphasized, there is generally no upper bound on $c(\gamma)$. On the other hand, due to the nested hierarchy of these events ($\forall \lambda, \gamma \leq \gamma' : A_\lambda(\gamma) \subset A_\lambda(\gamma')$) $c(\gamma)$ is necessarily an increasing function of γ.

Other fundamental properties are that $c(\gamma)$ must be convex and that if the process is conservative [Eq. (7)], then $c(\gamma)$ has the fixed point: $c(C_1) = C_1$, where C_1 is at the same time a singularity corresponding to the mean of the process and its codimension: at this point $c(\gamma)$ is tangent to the bisectrix. Figure 8(a) illustrates these properties of the codimension function $c(\gamma)$. This graphical representation helps also to estimate the limitations due to the finite size of a sample with the help of the "sampling dimension" D_s [Schertzer & Lovejoy, 1989b; Lavallée *et al.*, 1991] defined as being the scaling exponent of the number N_s of independent samples of resolution λ:

$$N_{s,\lambda} \approx \lambda^{D_s} \quad (18)$$

as well as the corresponding "sampling singularity" γ_s that is the almost sure maximal singularity present in a sample of sampling dimension D_s. This singularity γ_s has therefore a codimension equal to the overall effective dimension of sampling [see Fig. 8(b)]:

$$c(\gamma_s) = D + D_s = \Delta_s; \quad (19)$$

and it will be discussed further in Sec. 9.4.

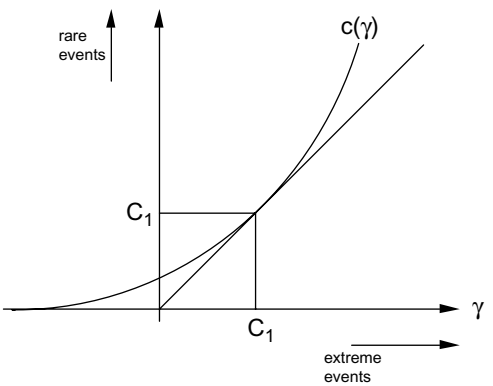

(a)

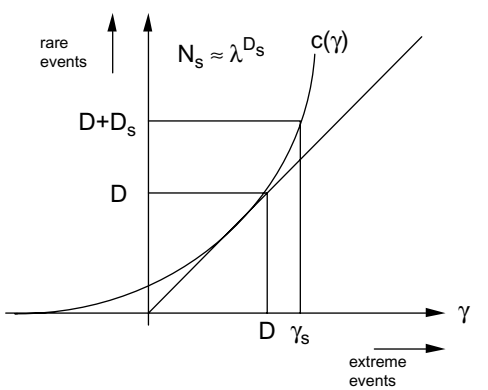

(b)

Fig. 8. A schematic illustration of a conserved multifractal, showing (a) the relations $c(C_1) = C_1$ and $c'(C_1) = 1$, where C_1 is the singularity of the mean, (b) how the sampling dimension imposes a maximum order of singularities γ's. From [Schertzer & Lovejoy, 1993].

4.2. *The multiscaling of moments $K(q)$ and the Legendre transformation*

Under fairly general conditions, a random variable can be specified by either its probability distribution or by (all) its statistical moments. For a non-negative random variable x, these two representations are linked by a Mellin transformation M, which is:

$$\begin{aligned} \langle x^{q-1} \rangle &= M(p) \\ &= \int_0^\infty x^{q-1} p(x) dx \quad (20) \\ p(x) &= M^{-1}(\langle x^{q-1} \rangle) \\ &= \frac{1}{2\pi i} \int_{c-i\infty}^{c+i\infty} \langle x^{q-1} \rangle x^{-q} dq \quad (21) \end{aligned}$$

(essentially these are simply the Laplace and inverse Laplace transforms for the logs). In fact, if the moments increase slowly with q (when they satisfy the "Carleman criterion" — see [Feller, 1971]), only the knowledge of the integer order moments is sufficient. The relevance of the Carleman criterion for turbulence has been discussed in [Orszag, 1970], but in any case the full Mellin duality [Schertzer & Lovejoy, 1993; Schertzer *et al.*, 2002] will hold.

This is somewhat more general than the Legendre duality pointed out in [Parisi & Frisch, 1985], but we can check that the Legendre transform is the asymptotic ($\lambda \to \infty$) result linking the

corresponding exponents. Since the codimension $c(\gamma)$ is the scaling exponent of the probabilities, let us introduce the corresponding scaling moment function $K(q)$:

$$\langle \varepsilon_\lambda^q \rangle \approx \lambda^{K(q)}. \tag{22}$$

For large $\log \lambda$, we can use the saddle point approximation (Laplace's method, see for example [Bender & Orszag, 1978]) which yields asymptotic approximations to integrals of exponential form. One obtains that $K(q)$ is related to $c(\gamma)$ by:

$$\begin{aligned}\langle \varepsilon_\lambda^q \rangle &= \int d\Pr(\varepsilon_\lambda)\varepsilon_\lambda^q \sim \int d\Pr(\varepsilon_\lambda)\lambda^{q\gamma} \\ &= \int_{-\infty}^{\infty} \mathrm{Log}(\lambda) dc(\gamma)\lambda^{q\gamma}\lambda^{-c(\gamma)}\end{aligned} \tag{23}$$

which yields the asymptotic behavior ($\lambda \to \infty$):

$$\begin{aligned}\lambda \gg 1: \quad &\int_{-\infty}^{\infty} dc(\gamma) \mathrm{e}^{\mathrm{Log}(\lambda)(q\gamma - c(\gamma))} \\ &\propto \mathrm{e}^{\mathrm{Log}(\lambda)\mathrm{Max}_\gamma(q\gamma - c(\gamma))}\end{aligned} \tag{24}$$

as well as the prefactor, which we do not consider here. A similar expansion can be done for the inverse Mellin transform Eq. (21), and we have therefore the (involutive) Legendre duality for the exponents:

$$\begin{aligned}K(q) &= \max_\gamma \{q\gamma - c(\gamma)\} \\ &\Leftrightarrow c(\gamma) = \max_q \{q\gamma - K(q)\}.\end{aligned} \tag{25}$$

This demonstrates that both curves are convex (iterating twice the Legendre transform, a nonconvex curve yields its "convex hull"). One may note that the convexity of $K(q)$ follows from the fact that it is the "second Laplace, base λ characteristic function" of $\mathrm{Log}_\lambda(\varepsilon_\lambda)$. This duality also means that the curve $c(\gamma)$ is the envelop of the tangencies of $K(q)$ and conversely. Hence there is a simple one-to-one correspondence between moments and orders of singularities.

4.3. *Comparison of multifractal formalisms*

Until now, we rather used a codimension multifractal framework [Schertzer & Lovejoy, 1987, 1989a, 1992] rather than a dimension multifractal framework [Parisi & Frisch, 1985; Halsey *et al.*, 1986]. The latter was first introduced in order to explain the nonlinearity of the scaling exponents of the velocity structure functions (the statistical moments of the velocity increments) empirically observed in [Anselmet *et al.*, 1984]. Parisi and Frisch [1985] considered that the singularities of the velocity increments defined as local Holder exponents should be geometrically and rather deterministically distributed over embedded fractals. The $f(\alpha)$ formalism [Halsey *et al.*, 1986], which dealt with multifractal strange attractors, in many respects further emphasized this implicit nonrandom and geometric framework. At the notation level, a dimension formalism such as $f(\alpha)$ formalism is formally related to codimensions according to:

$$\alpha_D = D - \gamma; \quad f_D(\alpha_D) = D - c(\gamma). \tag{26}$$

This is without fundamental formal problems as far as $c(\gamma) < D$, although all these dimensions depend on the considered embedding dimension D, as emphasized by the corresponding subindex D. Similarly, the scaling exponent $\tau(q)$ of the partition function [Hentschel & Procaccia, 1983] is related to that of the moments as

$$\tau_D(q) = (q-1)D - K(q). \tag{27}$$

With the help of the so-called refined self-similar hypothesis [Kolmogorov, 1962; Obukhov, 1962], the velocity increment singularities can be linearly related to the singularities of the energy flux, therefore, we will keep the energy flux as the basic field to compare the formalisms. The geometric approach considers the following supports of singularities:

$$S_\lambda(\gamma) = \left\{ x \in E \,|\, \varepsilon_\lambda(x) = \lambda^\gamma \varepsilon_1 \right\} \tag{28}$$

which rather correspond to the boundary of the events $A_\lambda(\gamma)$, which are defined by an inequality sign [Eq. (17)] instead of an approximate equality, i.e. $S_\lambda(\gamma) = \partial A_\lambda(\gamma)$ for a given stochastic realization $\omega \in \Omega$. As a consequence, there is no compelling reason that the supports $S_\lambda(\gamma)$ should be hierarchically embedded, contrary to the events $A_\lambda(\gamma)$. There is neither a compelling reason that their (geometrical) codimensions should be convex and increasing with respect to the singularity γ. Therefore, Parisi and Frisch [1985] explicitly made the corresponding hypothesis. Another difference is the limits ($\lambda \to \infty$) that are considered. In the geometric approach, one rather considers the set of points $\underline{S}(\gamma)$ which has the given singularity γ for eventually all resolutions λ's (i.e. for large enough λ),

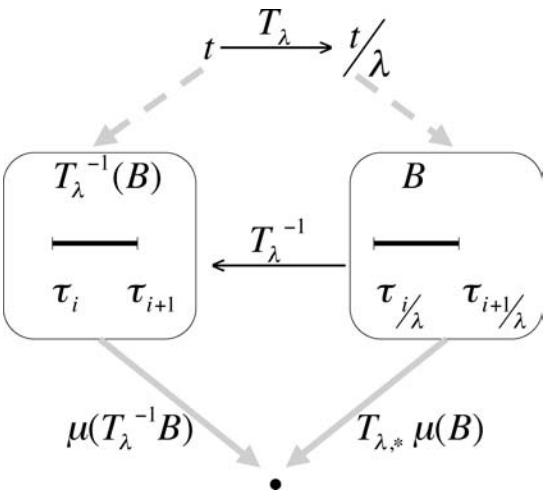

Fig. 9. Schematic diagram of the "pushforward" transform $T_{\lambda,*}$ of a (mathematical) measure μ due to a time contraction T_λ with a scale ratio λ (reproduced from [Schertzer *et al.*, 2010]).

therefore the limit inferior:

$$\underline{S}(\gamma) = \underline{\lim}_{\Lambda\to\infty} S_\Lambda(\lambda) \equiv \bigcup_\lambda \bigcap_{\Lambda>\lambda} S_\Lambda(\gamma) \qquad (29)$$

whereas, the asymptotic scaling of the probability [Eq. (16)] is rather related to the limit superior [Schertzer *et al.*, 2002]:

$$\overline{A}(\gamma) = \overline{\lim}_{\Lambda\to\infty} A_\Lambda(\gamma) \equiv \bigcap_\lambda \bigcup_{\Lambda>\lambda} A_\Lambda(\gamma) \qquad (30)$$

which corresponds to singularity γ for infinitely often resolutions λ's. Let us illustrate this question by pointing out that stochastic multifractal singularities are nonlocal [Schertzer & Lovejoy, 1992]. Indeed, when we add more and more cascade steps in a stochastic cascade, the singularity $\gamma_\lambda(x)$ at a given location x and increasing resolution λ undergoes a random walk (see e.g. Fig. 10), whereas a complete localization of the singularity would correspond to a pointwise limit: $\gamma(x) = \lim_{\lambda\to\infty} \gamma_\lambda(x)$. Therefore, the relevant limit notion is the upper limit [Eq. (30)] rather than the much more stringent lower limit [Eq. (29)]. For applications, this means that the multifractal field is *nonlocal*, and one cannot always track a given singularity value by locally refining the analysis of the field, e.g. with the help of wavelet analysis. This may yield spurious results. Parisi and Frisch [1985], Frisch [1995] acknowledged that within their formalism they could get *only* a bounded range of singularities (in fact $c(\gamma) < D$) for the so-called lognormal model. The practical importance of $c(\gamma) \geq D$ will be discussed in Sec. 9.

On the overall, we reviewed the fact that beyond their strong communality, various multifractal formalisms have important differences due to basic assumptions on the nature of the process (e.g. stochastic or deterministic), the hypothesis to be done is more or less stringent, but the resulting hierarchy of fractals can be also rather different: it

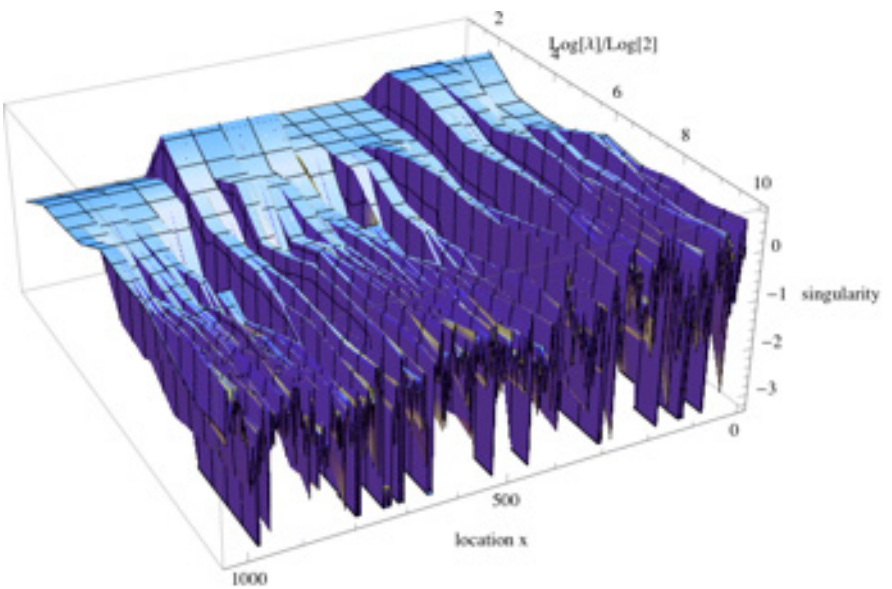

Fig. 10. Nonlocal development of singularities $\gamma_\lambda(x)$ (at location x and resolution L/λ) in a perspective view (along the number of steps $n = \mathrm{Log}_2[\lambda]$) in a discrete cascade of elementary scale ratio $\lambda_1 = 2$ and of universal parameters $\alpha = 1.5$, $C_1 = 0.5$ (see Sec. 6.3) over an overall ratio of scale Λ ($\geq \lambda$). It is rather obvious that for any given x, $\gamma_\lambda(x)$ fluctuates for increasing λ, contrary to the hypothesis of localness of singularity.

could be either defined for each realization or with looser probabilistic constraints.

5. Generators, Characteristic Functions and Multifactal Scale Symmetry

Discrete cascades, i.e. with scale ratio $\lambda \in \lambda_1^N = \{1, \lambda_1, \lambda_1^2, \lambda_1^3 \ldots\}$, point out that the ε_λ form a multiplicative group, a property that will be extended to continuous cascades. It is defined by the fact that a cascade from resolution 1 to Λ, can be obtained by multiplying a cascade from resolution 1 to $\lambda \leq \Lambda$ by a cascade from λ to Λ. Because, the latter correspond to a rescaled cascade from resolution 1 to Λ/λ (see Fig. 11), this group property corresponds to:

$$\forall\, \Lambda \geq \lambda \geq 1: \quad \varepsilon_\Lambda = \varepsilon_\lambda T_\lambda^*(\varepsilon'_{\Lambda/\lambda}) \tag{31}$$

where T_λ^* is the "pullback" transform for any function f:

$$\forall\, \underline{x} \in E: \quad T_\lambda^*(f)(\underline{x}) = f(T_\lambda(\underline{x})) \tag{32}$$

defined by a geometric point transform T_λ on the space E, on which ε_λ is defined (i.e. time and/or space). For the moment, up to Sec. 8 devoted to Generalized Scale Invariance, T_λ is taken to be trivial scale transformation, i.e. the isometric contraction:

$$T_\lambda(\underline{x}) = \frac{\underline{x}}{\lambda} \tag{33}$$

although it is already clear that the generality of the pullback transform will allow broad generalizations of the results obtained for the isometric contraction.

The name pullback evokes the fact that this transform acts in the opposite direction ("contravariantly") to that of the original transform T_λ. This general notion is particularly useful when dealing with differential equations [Schertzer *et al.*, 2012]. It is dual to the "pushforward" transform $T_{\lambda,*}$ acting ("covariantly") on measures according to the following duality equation:

$$\int f T_{\lambda,*}(d\mu) = \int T_\lambda^*(f) d\mu. \tag{34}$$

The pushforward transform $T_{\lambda,*}$ is particularly useful to mathematically deal with singular measures such as rain accumulation [Schertzer *et al.*, 2010]. It is rather easy to check that the (trivial) group property of the original transform T_λ extends to both the pullback and pushforward transforms and that both are linear respectively on vector spaces of functions and their dual spaces of measures.

Like for all one-parameter groups, we are interested to characterize the infinitesimal generator of a cascade, which can be stochastic. Loosely speaking this allows us to return to an additive group. Let us consider the generator Γ_λ of the cascade over a (noninfinitesimal) scale ratio λ defined by:

$$\varepsilon_\lambda = \exp(\Gamma_\lambda). \tag{35}$$

The additive group property corresponding to the multiplicative property displayed by Eq. (31) is:

$$\forall\, \Lambda \geq \lambda \geq 1: \quad \Gamma_\Lambda = \Gamma_\lambda T_\lambda^*(\Gamma'_{\Lambda/\lambda}). \tag{36}$$

The generator is well defined for any finite resolution λ, but its limit for asymptotically large

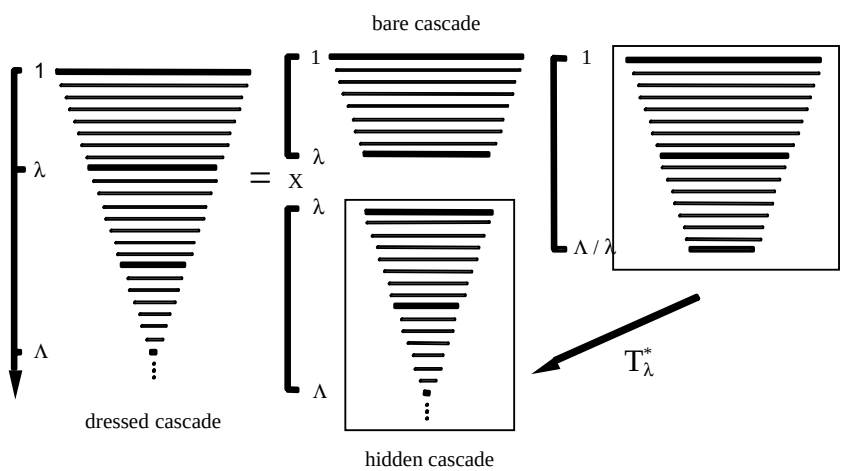

Fig. 11. A schematic diagram (horizontal segments schematically represent involved scales) showing a ("dressed") cascade from resolution 1 to a ("bare") cascade from resolution 1 to λ, multiplied by a ("hidden") cascade from resolution Λ/λ to Λ, which is the pushback transformed with the help of T_λ^* of a cascade constructed from resolution 1 to Λ/λ. The terminology of "dressed, bare and hidden" cascades will be discussed in Sec. 9.2. Reproduced from [Schertzer *et al.*, 2002].

resolutions is not trivial. This can be seen with the help of the moment scaling function $K(q)$, which gains a new and convenient meaning. Indeed, Eq. (22) can be rewritten under the form:

$$\langle e^{q\Gamma_\lambda} \rangle = Z_\lambda(q) = e^{K_\lambda(q)} \tag{37}$$

where $Z_\lambda(q)$ and $K_\lambda(q)$ are none other than respectively the (Laplace) first and second characteristic functions — or respectively the moment and cumulant generating functions — of the generator Γ_λ. This further shows that the characteristic function of Γ_λ, should be logarithmically divergent (with the scale ratio λ):

$$K_\lambda(q) = K(q)\mathrm{Log}\,\lambda \tag{38}$$

hence a nontrivial small scale limit of the generator Γ_λ.

We may now define fractal and multifractal symmetries in a very general and precise manner. Following [Lamperti, 1962], scale invariance for stochastic fractals is usually defined by:

$$\varepsilon(T_\lambda \underline{x}) \stackrel{d}{=} \lambda^H \varepsilon(\underline{x}) \tag{39}$$

where H is a given unique scaling exponent and ε can be an increment of random walk or field, as well as a measure. Considering the latter case, this can be rewritten with the help of the pushforward transform into a standard form of a symmetry S_λ:

$$S_\lambda \varepsilon \stackrel{d}{=} \varepsilon; \quad S_\lambda = \tilde{T}_\lambda \,\mathrm{o}\, T_{\lambda,*} \tag{40}$$

which corresponds to the product of a pushforward transform $T_{\lambda,*}$ by a codomain contraction, i.e. a contraction $\tilde{T}_\lambda$ on the space where ε is valued (up until now the real space $\Re$):

$$\tilde{T}_\lambda = \lambda^{-H}. \tag{41}$$

A multifractal symmetry is obtained for Eq. (40) as soon as $\tilde{T}_\lambda$ is no longer defined by a unique scaling exponent, but by a full set of singularities γ's:

$$\tilde{T}_\lambda \stackrel{d}{=} \lambda^{-\gamma} \equiv e^{-\Gamma_\lambda}. \tag{42}$$

Generalized scale invariance (Sec. 8) will further generalize this symmetry due to nonscalar anisotropic $\tilde{T}_\lambda$ and/or $T_{\lambda,*}$.

6. Universality

6.1. *The concept of universality*

The jump from fractals to multifractals is huge, since it corresponds to a jump from a unique dimension to an infinite hierarchy of dimensions. This is emphasized by the fact that there is only a convexity constraint on the nonlinear functions $K(q)$ and $c(\gamma)$, therefore *a priori* an infinity of parameters are required to determine a multifractal process. For obvious theoretical and empirical reasons, physics abhors infinity. This is the reason why in many different fields of physics the theme of *universality* appears: among the infinity of parameters, it may be possible that only a few are relevant. For instance, in critical phenomena most of the exponents describing phase transitions depend only on the dimensionality of the system. This is especially true as soon as we go beyond ideal systems to more realistic ones that should be robust to perturbations or self-interactions. Such perturbations or interactions may wash out many of the peculiarities of the theoretical model, retaining only some essential features. Loosely speaking, a theoretician may concoct a model for an isolated system depending on a very large number of parameters, but most natural systems are open and the resulting interactions can wash out most of the details, just leaving the (few) essentials. This was the basic idea of the Renormalizing Group approach [Wilson & Kogut, 1974].

The system can therefore be expected to converge to some *universal attractor*, in the sense that a whole class of models/processes with rather distinct parameters will be nevertheless attracted to the same process defined by only a small number of relevant parameters: the larger the basin of attraction, the more universal the attractor.

6.2. *Universality in multiplicative processes?*

The study of multiplicative random processes has a long history [Aitchison & Brown, 1957] going back to at least [McAlsister, 1879], who argued that multiplicative combinations of elementary errors would lead to lognormal distributions. Kapteyn [1903] generalized this somewhat and stated what came to be known as the "law of proportional effect", which has been frequently invoked since, particularly in biology and economics (see also [Lopez, 1979] for this law in the context of rain). This law was almost invariably used to justify the use of lognormal distributions i.e. it was tacitly assumed that the lognormal was a universal attractor for multiplicative processes. Although Kolmogorov [1962], Obukhov [1962] did not explicitly give the law of proportional effect as motivation, it was almost certainly

the reason why they suggested a lognormal distribution for the energy dissipation in turbulence. This claim seemed to be secured by the explicit "lognormal" cascade model developed in [Yaglom, 1966]. The claim of universality of the lognormal model was first criticized in [Orszag, 1970] and then in [Mandelbrot, 1974].

Whereas Orszag's criticism was on the grounds that the (infinite) hierarchy of integer order moments would not determine a lognormal process, Mandelbrot's criticism was based on the fact that even if the cascade process were lognormal at each finite step, that in the small scale limit, the spatial averages would *not* be lognormal. This limit already poses a nontrivial mathematical problem, since it corresponds to a weak limit of random measures [Kahane, 1985], as discussed in Sec. 9.1. Furthermore, since the particularities of the discrete models (e.g. the α-model) remain at each scale, therefore in its small-scale limit, this lead to the opposite claim: that multiplicative cascades do not admit *any* universal behavior [Mandelbrot, 1989, 1991; Gupta & Waymire, 1993].

6.3. *Universal multifractals and the multiplicative central limit theorem*

As long as we keep the total *range of scale fixed and finite mixing* (by multiplying them) *independent processes* of the *same type* (identical distribution, therefore the same codimension function $c(\gamma)$ and scaling moment function $K(q)$), and *then* take the limit $\Lambda \to \infty$ [Schertzer & Lovejoy, 1987, 1988], we avoid the difficulties that we mentioned above and a totally different limiting problem is obtained.

For instance, this may correspond to a (renormalized) *densification* of the excited scales by introducing more and more intermediate scales (see Fig. 12), e.g. to obtain a continuous scale cascade model as discussed in Sec. 7. Alternatively, we may also consider the (renormalized) nonlinear mixing of identically independently distributed (i.i.d.) cascade models which correspond to their multiplication. In both cases, we first look for the cascade processes that are *stable* under either nonlinear mixing or densification, then to their *attractivity* and their domain of attraction. Stable cascades are the fixed points $\varepsilon_\lambda \stackrel{d}{=} \varepsilon_\lambda^{(1)}$ of:

$$\lambda^{-a_1}\varepsilon_\lambda = \prod_{i=1,N} (\lambda^{-a_N}\varepsilon_\lambda^{(i)})^{1/b_N} \qquad (43)$$

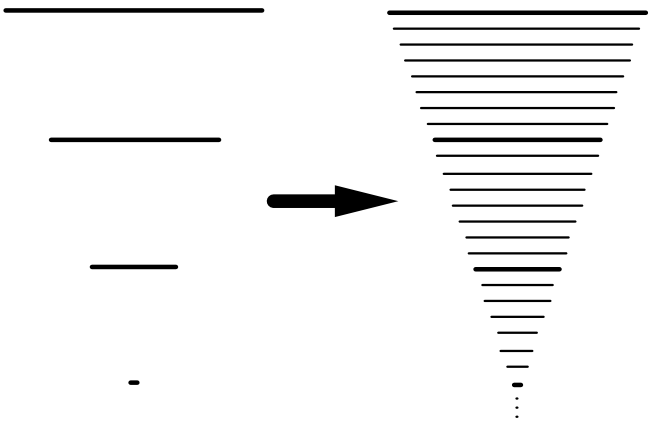

Fig. 12. Scheme of densification of scales: each horizontal line schematizes to a step of the cascade from large to small scales (up to bottom). Scale densification of a cascade (left, with a rather large elementary scale ratio) corresponds to more and more intermediate steps (right, with a smaller elementary ratio). From [Schertzer & Lovejoy, 1997].

where a_N, b_N (with the nonrestrictive choice $b_1 = 1$) are renormalizing constants and $\varepsilon_\lambda^{(i)}$ are N independently identically distributed cascade processes on the same range of scales with an overall resolution λ for nonlinear mixing or $\varepsilon_\lambda^{(i)}$ are the successive elementary cascade steps (of elementary resolution λ) for a scale densification over the same scale ratio λ. Secondly, one has to check that these stable points are attractive over a given domain of processes.

A multiplicative central limit theorem [Schertzer & Lovejoy, 1997] is obtained with the help of the cascade generator. Indeed, Eq. (43) corresponds to the generalized (additive) stability problem [Lévy, 1925, 1937; Gnedenko, 1943; Gnedenko & Kolmogorov, 1954], i.e. the following fixed point:

$$\Gamma_\lambda - a_1 \mathrm{Log}\,\lambda = \sum_{i=1}^{N} \frac{\Gamma_\lambda^{(i)} - a_N \mathrm{Log}\,\lambda}{b_N}. \qquad (44)$$

For instance, iteration of Eq. (43) or (44) shows that the b_N's form a multiplicative group with $a_N = a_1$:

$$b_{NM} = b_N b_M \qquad (45)$$

and one then may introduce the exponent α to generate this group:

$$b_N = N^{1/\alpha}. \qquad (46)$$

On the other hand, taking ensemble averages of both sides of Eq. (43) one obtains that the scaling moment function $K(q)$ of ε_λ is the fixed point

$K(q) = K^{(1)}(q)$ of:

$$K(q) - a_1 q = N\left[K^{(1)}\left(\frac{q}{b_N}\right) - \frac{a_N q}{b_N}\right] \quad (47)$$

which yields the solutions:

$$K(q) = cq^{\alpha} + a_1 q. \quad (48)$$

Attractivity is rather immediate. Indeed, let us consider the following $K^{(i)}(q)$ (with $\beta > \alpha$):

$$\begin{aligned} K^{(i)}(q) &= K(q) + O(q^{\beta}) \\ &= cq^{\alpha} + a_1 q + O(q^{\beta}) \end{aligned} \quad (49)$$

we have therefore:

$$K(q) - a_1 q = \lim_{N\to\infty} N\left[K^{(1)}\left(\frac{q}{b_N}\right) - \frac{a_N q}{b_N}\right] \quad (50)$$

and therefore the corresponding ε_λ is attractive:

$$\lambda^{-a_1}\varepsilon_\lambda = \lim_{N\to\infty} \prod_{i=1,N} (\lambda^{-a_N}\varepsilon_\lambda^{(i)})^{1/b_N}. \quad (51)$$

Finally, with the help of the constraint $K(1) = 0$ of a conservative field, Eq. (48) yields the following scaling moment function of a conservative universal multifractal [Schertzer & Lovejoy, 1987] (see Fig. 13 for an illustration):

$$K(q) = \frac{C_1}{\alpha - 1}(q^{\alpha} - q); \quad 0 \le \alpha \le 2 \quad (52)$$

where C_1 is the singularity of the mean field ($q = 1$), which with the help of the Legendre transform is defined by:

$$C_1 = \frac{d}{dq}K(q)\bigg|_{q=1}. \quad (53)$$

The constraint on α mentioned in Eq. (52) results from the requirement that the (first) characteristic function $Z_\lambda(q)$ [Eq. (37)] of the generator should be positive definite so as to be a Mellin transform of a probability (according to the Schoenberg's theorem [Schoenberg, 1938], which complements the Bochner's theorem [Bochner, 1955] for the Laplace transform). The two extreme cases correspond respectively to the (uni/mono) fractal β-model ($\alpha = 0$) and the lognormal model ($\alpha = 2$), whereas the case $\alpha = 1$ is derived from Eq. (52) with $\alpha \to 1$:

$$K(q) = C_1 q \mathrm{Log}\, q; \quad \alpha = 1. \quad (54)$$

Equation (52) shows that for $0 < \alpha < 2$ the generator Γ_λ follows an "extremely asymmetric" or "skewed" Levy distribution (i.e. its skewness parameter $\beta = -1$) so that the fat tail (power-law tail) is present only for negative fluctuations, otherwise the field ε_λ will have divergent statistical moments ($K(q) = \infty$) for all positive order q. Nevertheless, all the negative statistical moments of ε_λ diverge, which is neither a problem, nor surprising due to its frequent extremely low or even zero values (especially for the β-model).

Due to the fact that q^{α}/α and $\gamma^{\alpha'}/\alpha'$ are Legendre duals for $(1/\alpha) + (1/\alpha') = 1$, one obtains

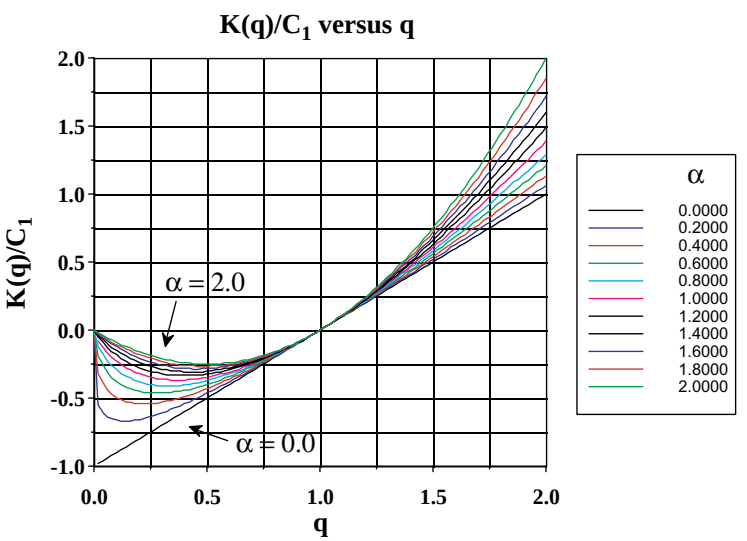

Fig. 13. The universal multifractal moment scaling exponent $K(q)$ normalized by C_1. They lie between the parabolic ($\alpha = 2$) "log-normal" model and the linear ($\alpha = 0$) β model.

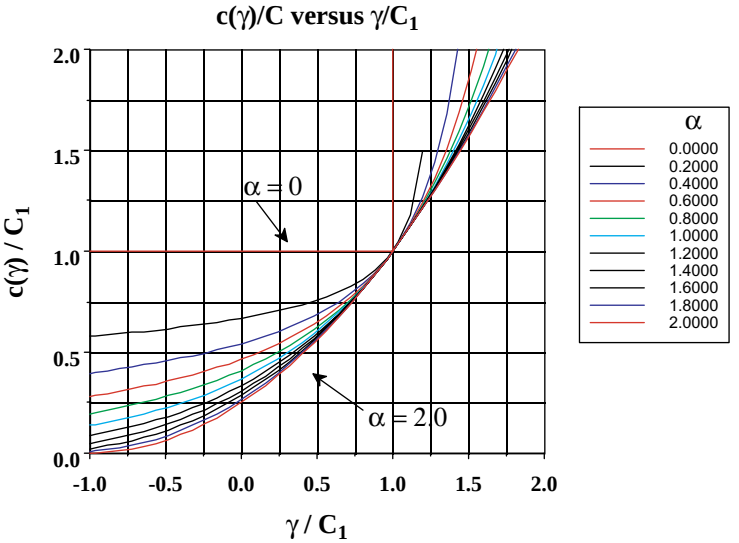

Fig. 14. The universal multifractal probability exponent $c(\gamma/C_1)$ normalized by C_1. They lie between the parabolic ($\alpha = 2$) "log-normal" model and the bilinear ($\alpha = 0$) β model.

from Eq. (52):

$$c(\gamma) = C_1 \left(\frac{\gamma}{C_1 \alpha'} + \frac{1}{\alpha} \right)^{\alpha'} ; \quad \frac{1}{\alpha} + \frac{1}{\alpha'} = 1 \qquad (55)$$

see Figs. 13 and 14 for illustration of the parameter sensitivity of the scaling moment and codimension functions.

7. Continuous Scale or "Infinitely Divisible" Cascades

7.1. *The limitations of discrete scale cascades*

An important consequence of universality is the possibility of starting with a discrete cascade model (e.g. one with an elementary scale ratio $\lambda_1 = 2$) and with the help of a scale densification to obtain a continuous in-scale process $\lambda_1 \to 1$. Such cascades are necessary since physically we expect real systems to involve a continuum of scales and there is usually no physically based quantization rule that would restrict scale ratios to integer values. Furthermore the discrete models involve a hierarchical splitting rule of structures into substructures which is based on a notion of distance which is not a metric, but rather an "ultra-metric". More precisely, it corresponds to the λ-adic ultrametric: the distance between two structures at a given level of a discrete cascade process is defined by the level of the cascade where they first share a common ancestor, i.e. not by the usual distance. This implies that the distance between the centers of two contiguous eddies is not uniformly distributed. Since all the statistical interrelations between different structures depend on this ultra-metric, not on the usual metric, this has drastic consequences. In particular, there is no hope of obtaining a (statistically) translation invariant cascade, since such invariance depends on the metric, not the ultra-metric.

In summary, discrete cascades are useful for grasping many of the fundamentals, but one has to avoid being blocked by their artifacts. As a final note on discrete scale cascades, let us emphasize that almost all rigorous mathematical results on cascade processes have been derived in this restricted framework; this is not only because it is convenient, but also for complex historical reasons — including the debate on universality discussed above. As a consequence, the issue of continuous scale or infinitely divisible cascades has not been discussed enough.

7.2. *Continuous scale cascades and their generators*

The general idea of cascades as one-parameter multiplicative groups discussed in Sec. 5, especially Eq. (31) becomes essential for continuous scale cascades. For instance, the corresponding additive property for generators [Eq. (36)] show that they should be infinitely divisible, i.e. they can be divided into smaller and smaller additive components. On the other hand, we also saw that scaling requires a logarithmic divergence of the generator.

For a concrete and generic example, let us consider the case of universal multifractals (Sec. 6.3), whose generators are not only infinitely divisible, but also stable and attractive. They are therefore robust under nonlinear interactions. To satisfy the logarithmic divergence their generators [Eq. (33)] should be (colored) stable Lévy noises [Schertzer & Lovejoy, 1987] obtained by a fractional integration over a given "subgenerator", which is white Lévy noise $\gamma_0^{(\alpha)}$ with a Lévy stability index α and furthermore "unitary" in the sense that its (Laplace) second characteristic function is:

$$K_0(q) = \text{sign}(\alpha - 1)q^{\alpha} \cdot 1_{q \geq 0} + \infty \cdot 1_{q<0} \quad (56)$$

which means that $\gamma_0^{(\alpha)}$ is extremely asymmetric [Schertzer *et al.*, 1988] for $\alpha < 2$, i.e. with a skewness $\beta = -1$, to have only strong negative extremes. This is no longer relevant for the Gaussian case ($\alpha = 2$), which is necessarily symmetric ($\beta = 0, K(q) = q^2$) and has therefore no divergence for $q < 0$. Figure 15 compares the subgenerators in the $\alpha < 2$, $\alpha = 2$ cases.

This can be seen under a (fractional) differential form of order D/α' using a fractional power of the Laplacian $\Delta_{\underline{x}}$ (with a scale resolution L/λ):

$$-(-\Delta_{\underline{x},\lambda})^{D/2\alpha'}\Gamma_\lambda(\underline{x}) \approx \gamma_0^{(\alpha)}(\underline{x}) \quad (57)$$

or under the corresponding and more explicit (fractional) integration form:

$$\Gamma_\lambda(\underline{x}) = \left|\frac{\text{var}(\alpha)}{m_{D-1}(\partial B_L)}\right|^{1/\alpha} \int_{B_L \setminus B_{L/\lambda}(\underline{x})} \frac{d^D\gamma_0^{(\alpha)}(\underline{x}')}{|\underline{x} - \underline{x}'|^{D/\alpha}} - \text{var}(\alpha)\text{Log}\,\lambda;$$

$$\text{var}(\alpha) = \frac{C_1}{\alpha - 1} \quad (58)$$

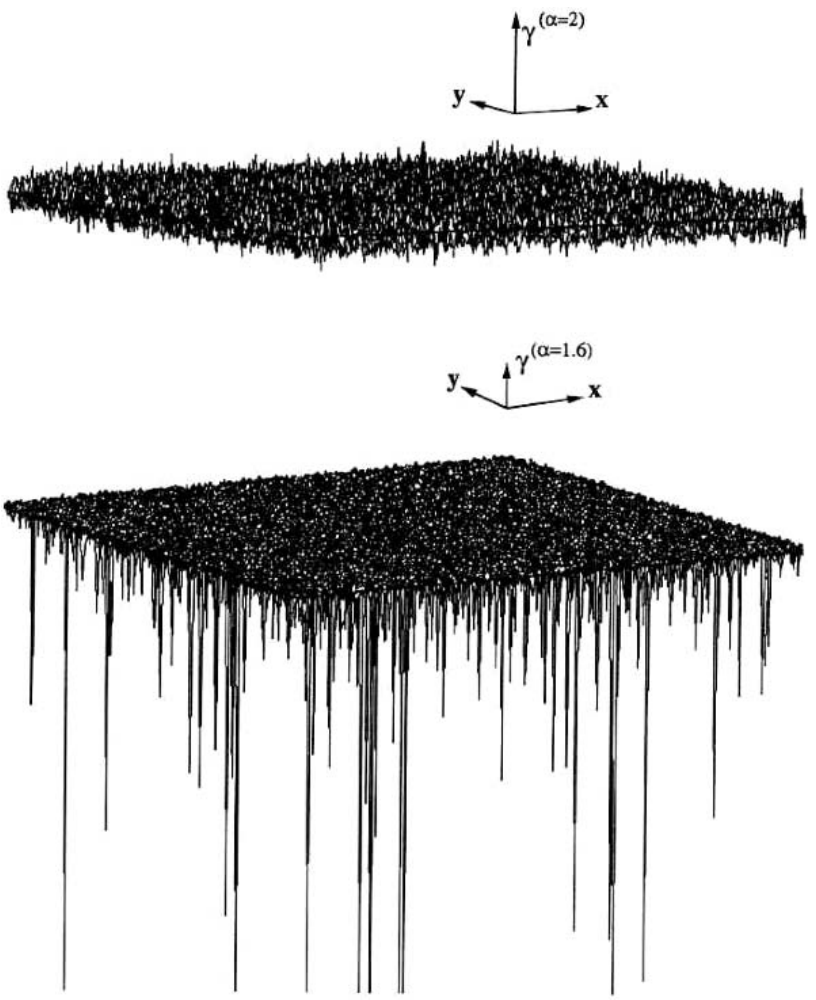

Fig. 15. A schematic showing a gaussian and extremal Levy subgenerator (with $\alpha = 1.6$); note that there are extremes only for the negative fluctuations. From [Wilson, 1991].

where $B_L(\underline{x})$ is the ball of center $\underline{x}$ and size L (which could be arbitrarily chosen), $m_{D-1}(\partial B_L)$ is the $(D-1)$-dimensional measure of its (hyper-)surface ∂B_L. For isotropic cases, $B_L(\underline{x}) = \{\underline{x}' \,|\, |\underline{x} - \underline{x}'| \leq L/2\}$, $B_L \backslash B_{L/\lambda}(\underline{x}) = \{\underline{x}' \,|\, L/2\lambda < |\underline{x} - \underline{x}'| \leq L/2\}$ and $m_{D-1}(\partial B_L) = 2(L/2)^{D-1}\pi^{D/2}/\Gamma_E(D/2)$ (where Γ_E is the Euler Gamma function). In order to get some convergent moments (finite $K(q)$), the subgenerator $\gamma_0^{(\alpha)}$ must be extremely assymmetrical. It is also interesting to note that ε_λ due to Eq. (58) is the solution of the following differential equation:

$$d\varepsilon_\lambda = \varepsilon_\lambda d\gamma_\lambda \tag{59}$$

where $d\gamma_\lambda$ is the infinitesimal generator of the multiplicative group of ε_λ:

$$d\gamma_\lambda = \left| \frac{\mathrm{var}(\alpha)}{m_{D-1}(\partial B_L)} \right|^{1/\alpha} \int_{\partial B_{L/\lambda}(\underline{x})} \frac{d^D \gamma_0^{(\alpha)}(\underline{x}')}{|\underline{x} - \underline{x}'|^{D/\alpha}} \tag{60}$$

where $\mathrm{var}(\alpha)$ corresponds to a generalization of the (quadratic) variation of a (semi-) martingale (e.g. [Metivier, 1982]) and this explains why:

$$d\gamma_\lambda - d\Gamma_\lambda = \frac{\mathrm{var}(\alpha) d\lambda}{\lambda}. \tag{61}$$

7.3. *Nonconservative multifractals and the Fractionally Integrated Flux model (FIF)*

Integration of Eq. (59) [or equivalent use of the generator defined by Eq. (58)] yields a conservative field

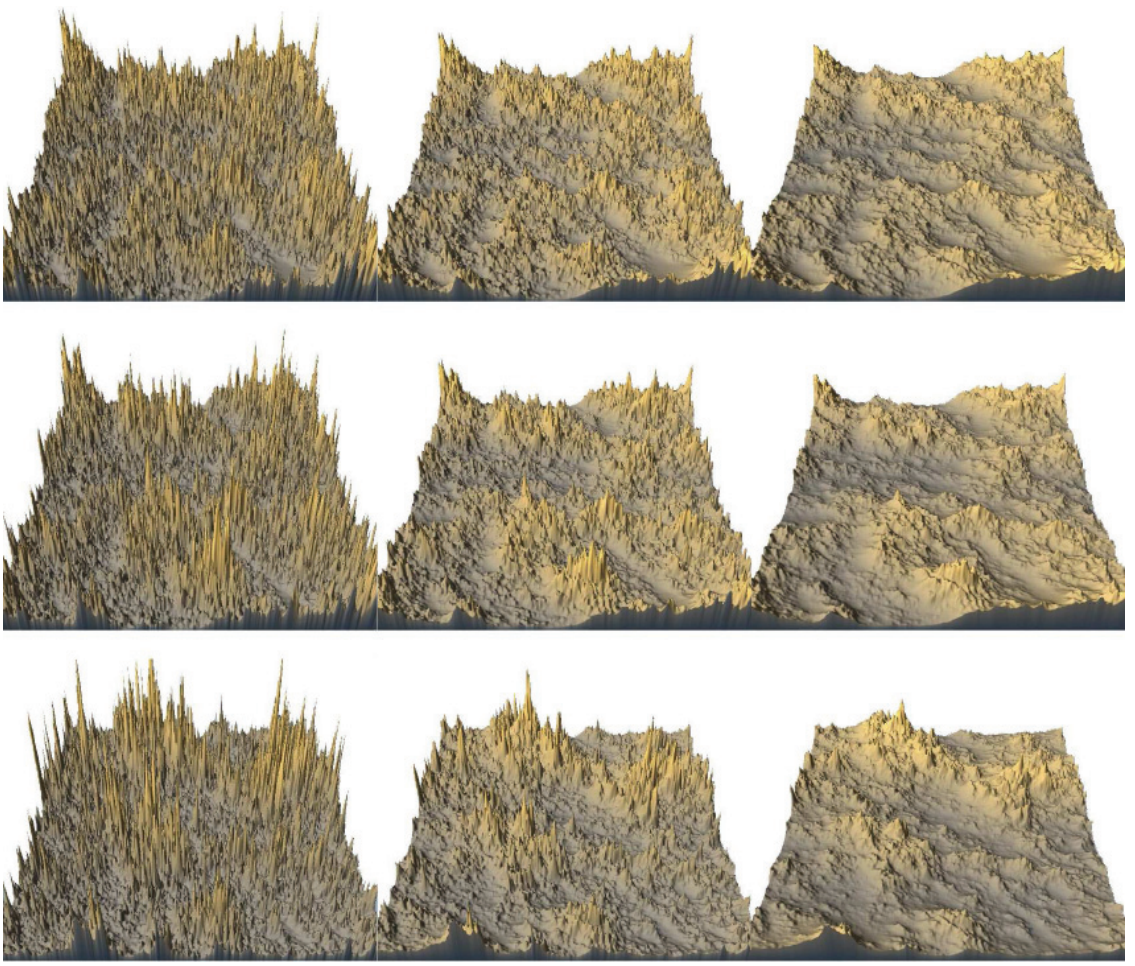

Fig. 16. Isotropic (i.e. self-similar) multifractal simulations showing the effect of varying the parameters α and H ($C_1 = 0.1$ in all cases). (From left to right) $H = 0.2$, 0.5 and 0.8. (From top to bottom) $\alpha = 1.1$, 1.5 and 1.8. As H increases, the fields become smoother and as α decreases, one notices more and more prominent "holes" (i.e. low smooth regions). The realistic values for topography ($\alpha = 1.79$, $C_1 = 0.12$, $H = 0.7$) correspond to the two lower right-hand simulations. All the simulations have the same random seed. Reproduced from [Gagnon *et al.*, 2006].

ε_λ, which is not always a desirable property. The classic example of such nonconsevative processes is the turbulent velocity field; in Kolmogorov three-dimensional isotropic turbulence, whose structure function is not scale invariant: $\langle \Delta v^2(L/\lambda)\rangle \approx \lambda^{-2H}\langle \Delta v^2(L)\rangle$, with: $H = 1/3$. This constraint is easily satisfied with the help of a fractional integration of order H:

$$\nu_\lambda(\underline{x}) \propto \int_{B_L \setminus B_{L/\lambda}(\underline{x})} \frac{d^D\varepsilon(\underline{x}')}{|\underline{x}-\underline{x}'|^{D-H}}. \qquad (62)$$

In the framework of this Fractionally Integrated Flux model [Schertzer *et al.*, 1997], the singularities are redistributed with an average shift of $-H$ as seen on the structure functions, i.e. the statistical moments of the increments $\Delta\nu(\underline{x},\underline{x}') = |\nu(\underline{x}) - \nu(\underline{x}')|$:

$$\langle |\nu(\underline{x}) - \nu(\underline{x}')|^q\rangle \propto |\underline{x}-\underline{x}'|^{qH-K(q)}. \qquad (63)$$

These increments have therefore a scale dependent mean, with $H \neq 0$ as scaling exponent (see Figs. 16 and 17). Figures 15 and 18 display the effect of changing the order of this scale invariant smoothing of order H. The convolution involved in Eq. (63) corresponds to a fractional integration of (fractional) order H over ε. However, there is not a unique definition of such a noninteger integration. For instance, to respect causality for processes in time, the corresponding kernel or Green function should be totally asymmetric in order not to

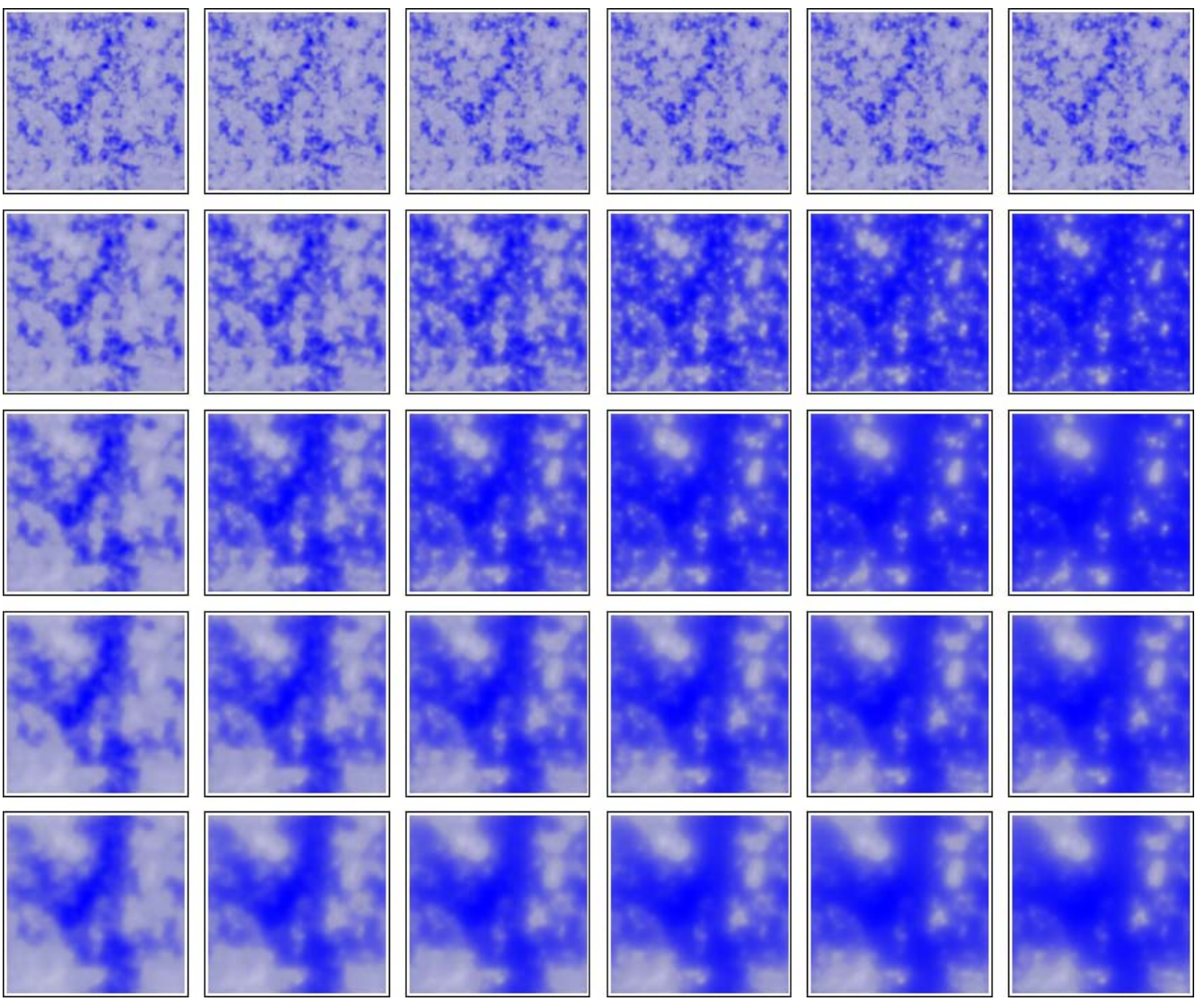

Fig. 17. All simulations have $H = 0.35$ (this is a scale invariant smoothing, see Sec. 7.3). The parameter C1 increases from 0.05 to 0.8 in steps of 0.15 from left to right and α increases from 0.4 from top to bottom in units of 0.4 to 2.0 (bottom).

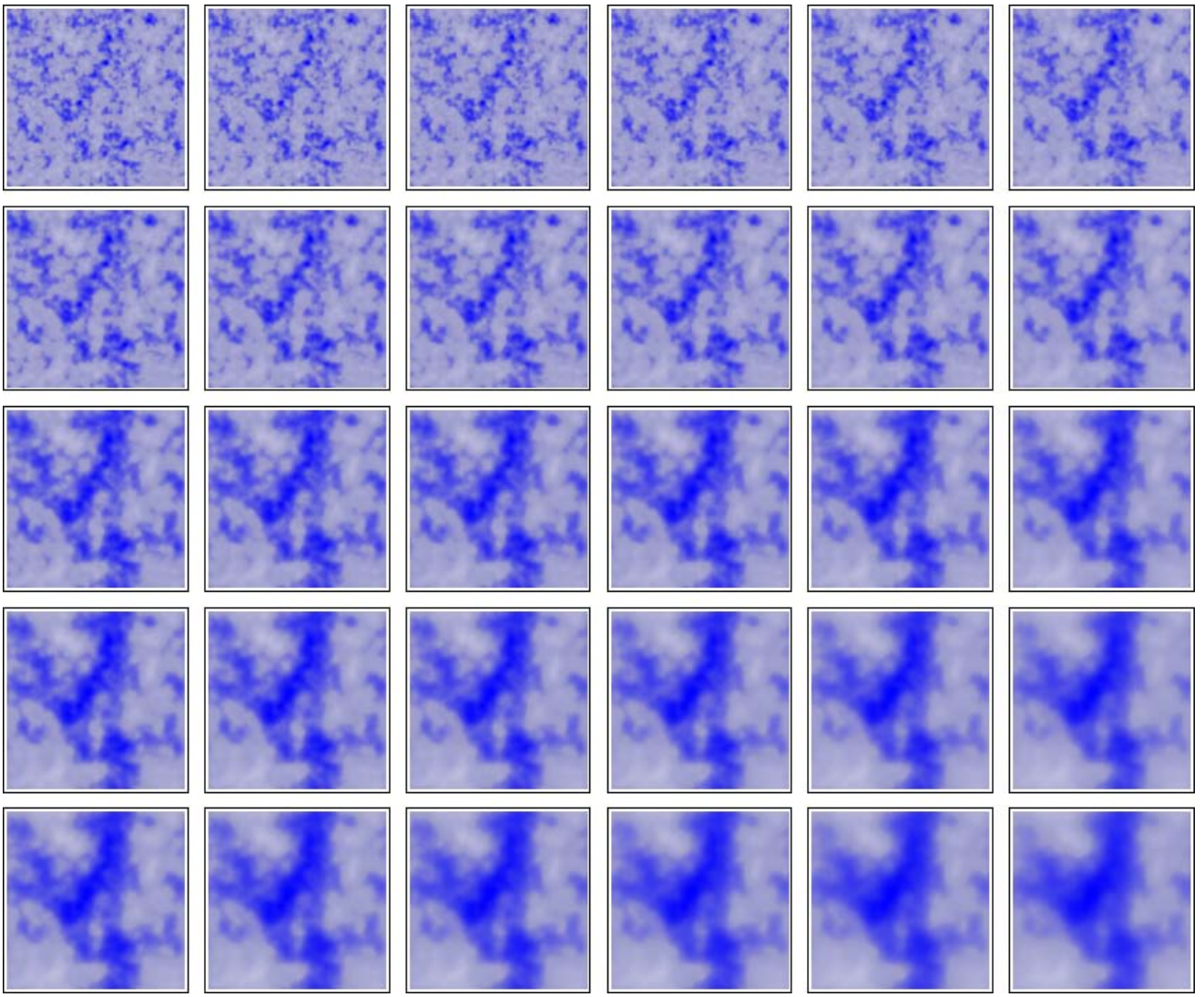

Fig. 18. All simulations have $C_1 = 0.05$. The parameter H increases from 0.05 to 0.8 in steps of 0.15 from left to right and α increases from 0.4 from top to bottom in units of 0.4 to 2.0 (bottom).

integrate over the future [Marsan *et al.*, 1996]. This is particularly important for predictability studies [Schertzer & Lovejoy, 2004a] and multifractal forecasts [Macor *et al.*, 2007]. In fact, it suffices to introduce a Heaviside function ($1_{t\geq 0}$) as a prefactor to the noncausal kernel to obtain a causal Green function $g(t,t')$, e.g.:

$$g(t,t') = \frac{1_{t-t'\geq 0}}{|t-t'|^{D-H}}. \qquad (64)$$

Furthermore, "delocalized" kernels can be defined for space-time processes to have a given scaling exponent $D-H$ and at the same time singularities (e.g. poles) in their Fourier transforms that generate waves. This will be discussed further in the next section that introduces the necessary concept and tools of Generalized Scale Invariance.

8. Generalized Scale Invariance (GSI)

8.1. *Generalized scales*

Up until now we have considered "self-similar" fractals and multifractals i.e. geometric sets and fields that are not only scaling, but also statistically rotationally invariant. However real world systems are not isotropic so that it is important to generalize this to strongly anisotropic systems. The resulting "Generalized Scale Invariance" (GSI) was actually motivated by the need to account for the strong scaling stratification of the atmosphere [Schertzer & Lovejoy, 1985b, 1985a]: Fig. 19 gives a (scaling) anisotropic version of the isotropic cascade scheme (Fig. 5) originally developed to model atmospheric stratification, which has gained increasing empirical confirmation (Fig. 20) with the help of various

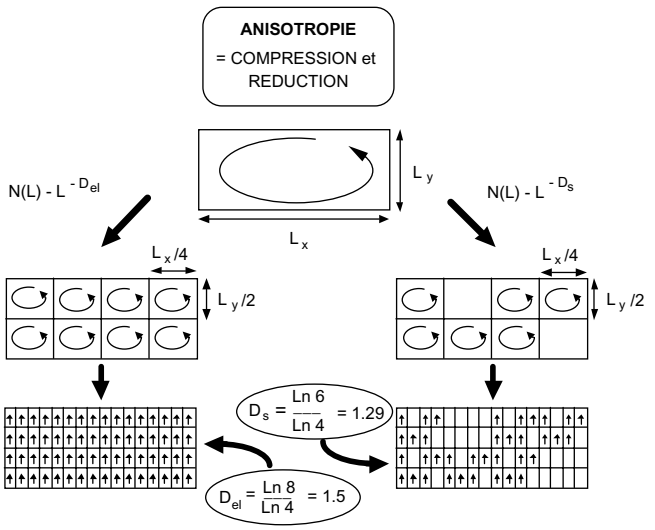

Fig. 19. Anisotropic cascade scheme: compare with Fig. 5. From [Schertzer *et al.*, 2002].

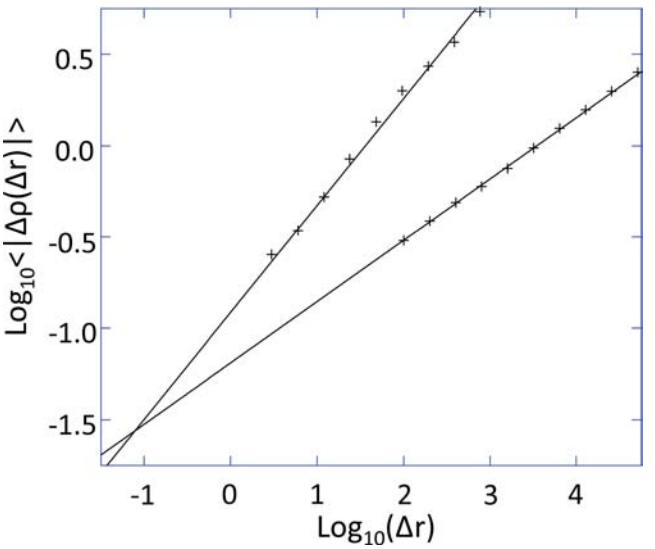

Fig. 20. The symbols show the mean absolute fluctuations (the first order structure functions) of the lidar backscatter ratio ρ (a surrogate for the passive scalar aerosol density). The points near the shallow slope (slope 1/3, Kolmogorov value) are the horizontal fluctuations, the points near the steeper line (slope 3/5, Bolgiano–Obukhov value) are for the vertical fluctuations. The averages are over an ensemble of nine vertical airborne lidar cross-sections spanning the range of ≈ 100 m–100 km in the horizontal and 3 m–4 km in the vertical. Δr is either the vertical or horizontal distance measured in meters. The lines have the theoretical slopes 3/5, 1/3, they intersect at the sphero-scale here graphically estimated from the intersection point as ≈ 10 cm. From [Lilley *et al.*, 2004].

atmospheric measurements [Chigirinskaya *et al.*, 1994; Lazarev *et al.*, 1994; Lilley *et al.*, 2004; Lovejoy & Schertzer, 2007; Lovejoy *et al.*, 2007].

The usual approach to scaling is to first posit (statistical) isotropy and only then to consider scaling. This approach is so prevalent that the terms "scaling" and "self-similarity" are frequently used interchangeably! The most famous example of this is Kolmogorov's hypothesis of "local isotropy" from which he derived the $k^{-5/3}$ spectrum for the wind fluctuations (k is a wavenumber). The GSI approach is the converse: it first posits scale invariance (scaling), as the main symmetry and then considers the remaining nontrivial symmetries. One may easily check that the type of anisotropic construction shown in Fig. 19 reproduces itself from scale to scale without introducing any characteristic scale. Since it involves scaling anisotropy in fixed directions, it is called "self-affinity". This anisotropic scheme is apparently the first explicit model of a physical system involving a fundamental self-affine fractal mechanism [Schertzer & Lovejoy, 1984, 1985a].

GSI corresponds to the fact that the contraction operators T_λ [Eq. (33)] or $\tilde{T}_\lambda$ [Eq. (34)], which define the scaling symmetry [Eq. (40)], are no longer isotropic [Eq. (33)] nor merely scalar [Eq. (41)]. For simplicity sake we first focus on the anisotropy of T_λ, keeping $\tilde{T}_\lambda$ scalar, but *mutadis muntandis* the same apply to an anisotropic $\tilde{T}_\lambda$ and a scalar T_λ, and finally both being anisotropic. In an abstract manner, T_λ is a generalized contraction on a vector space E, if it is a one-parameter (semi-) group for the positive real scale ratio λ ($\lambda \geq 1$ for a semigroup), i.e.

$$\forall\, \lambda, \lambda' \in R^+: \quad T_{\lambda'} \circ T_\lambda = T_{\lambda' \lambda} \tag{65}$$

and admits a generalized scale denoted $\|\underline{x}\|$ (to distinguish it from the usual Euclidean metric $|\underline{x}|$), which satisfies the following three properties [Schertzer *et al.*, 1999] further to that of being non-negative:

(i) *nondegeneracy*, i.e.

$$\|\underline{x}\| = 0 \Leftrightarrow \underline{x} = \underline{0} \tag{66}$$

(ii) *linearity* with the contraction parameter $1/\lambda$, i.e.

$$\forall\, \underline{x} \in E,\ \forall\, \lambda \in R^+:\ T_\lambda \|\underline{x}\| \equiv \|T_\lambda \cdot \underline{x}\| = \lambda^{-1} \|\underline{x}\| \tag{67}$$

(iii) balls defined by this scale, i.e.

$$B_\ell = \{\underline{x} \,|\, \|\underline{x}\| \leq \ell\} \tag{68}$$

must be *strictly decreasing* with the contraction T_λ:

$$\forall L \in R^+, \ \forall \lambda > 1: \quad B_{L/\lambda} \equiv T_\lambda(B_L) \subset B_L \tag{69}$$

and therefore:

$$\forall L \in R^+, \ \forall \lambda' \geq \lambda \geq 1: \quad B_{L/\lambda'} \subset B_{L/\lambda}. \tag{70}$$

The usual Euclidean norm $|\underline{x}|$ of a metric space is the scale associated to the isotropic contraction $T_\lambda \underline{x} = \underline{x}/\lambda$. The two first properties are rather identical to those of a norm, whereas the last one is weaker than the triangular inequality, which is required for a norm.

8.2. *Linear GSI*

This corresponds to the simplest, but already startling generalization of scale invariance: T_λ is no longer a scalar transform, but remains a linear transform. In this case, the group property Eq. (65) corresponds to the fact that this linear transform is power law of a given linear (infinitesimal) generator G:

$$T_\lambda = \lambda^{-G} \equiv \exp(-G \cdot \mathrm{Log}(\lambda)). \tag{71}$$

This can be easily understood with the help of the corresponding matrices. This "integral" form is equivalent to the following differential one:

$$\lambda \frac{d}{d\lambda} T_\lambda = -G \circ T_\lambda. \tag{72}$$

This differential equation also governs the evolution ($\lambda \geq 1$) of the point $x_\lambda = T_\lambda x_1$, whose trajectory starts from an initial ball B_L and crosses the balls $B_{L/\lambda}$. The classical isotropic contraction corresponds to the scalar case: $G = 1$, where 1 denotes the identity application. The next simplest case corresponds to the "self-affine" case [Mandelbrot, 1985], where G is diagonalizable, with real eigenvalues μ_i and eigenvectors e^i. Figure 21 shows that "zooming" into such a multifractal leads to systematic changes in shapes of the basic structures. This graphically demonstrates the "phenomenological fallacy" [Lovejoy & Schertzer, 2007] in which differences in morphology are confounded with differences in mechanism. Figure 22 shows the effect of varying the "sphero-scale"; the scale where structures are roughly "roundish".

It is straightforward to check that for $\mathrm{Spec}(G) > 0$, where $\mathrm{Spec}(\cdot)$ denotes the spectrum, the scale can be defined for any given positive $0 < \alpha \leq \infty$ as:

$$\left\| \sum_i x_i e^i \right\| = \left(\sum_i \|x_i e^i\|^\alpha \right)^{1/\alpha} \tag{73}$$

with:

$$\forall i, x_i : \|x_i e^i\| = ||x_i|^{1/\mu_i} e^i| \tag{74}$$

where $|\cdot|$ is a given norm on the vector space. These equations are very convenient to define anisotropic processes, including space-time processes. Indeed, the Green functions defining either a generator or a FIF model could be defined either in the physical space or the Fourier space with the help of these scales, e.g. for a (causal) space-time process:

$$\begin{aligned} \hat{g}(\underline{k}, \underline{x}) &\equiv \int d^D \underline{x} dt e^{i(\underline{k}\,\underline{x} + \omega t)} g(x, t) \\ &= (i\omega + \|k\|^{H_t})^{-H/H_t} \end{aligned} \tag{75}$$

where H_t is the scaling anisotropy exponent between time and space. Furthermore, to obtain a pole, therefore waves, still keeping the same scaling behavior, it suffices to consider [Lovejoy *et al.*, 2008b]:

$$\hat{g}_w(\underline{k}, \underline{x}) = (i\omega - \|k\|^{H_t})^{-H/H_t} \tag{76}$$

as well any weighted products of $g(\underline{k}, \underline{x})$ and $g_w(\underline{k}, \underline{x})$, i.e. weighted convolutions of $g(\underline{k}, \underline{x})$ and $g_w(\underline{k}, \underline{x})$. This already provides a wide, although presumably not exhaustive framework to study turbulence and waves. Equation (74) also confirms that the transformation of the norm $|\cdot|$ to the generalized scale $|\cdot|$ corresponds to a nonlinear transform (except for the scalar case: $G = 1$), which may be defined as:

$$x_i \to \mathrm{sign}(x_i)|x_i|^{1/\mu_i}. \tag{77}$$

Nevertheless, the most interesting cases correspond to complex eigenvalues, which obviously introduce rotations, and nondiagonalizable generators (Jordan matrices). This is illustrated in Figs. 23 and 24 for a two-dimensional generator G. The reality of the eigenvalues corresponds to:

$$a^2 = \left(\frac{\mathrm{Tr}(G)}{2} \right)^2 - \mathrm{Det}(G) > 0 \tag{78}$$

and a dominant stratification effect, whereas $a^2 < 0$ corresponds to a dominant rotation effect. For

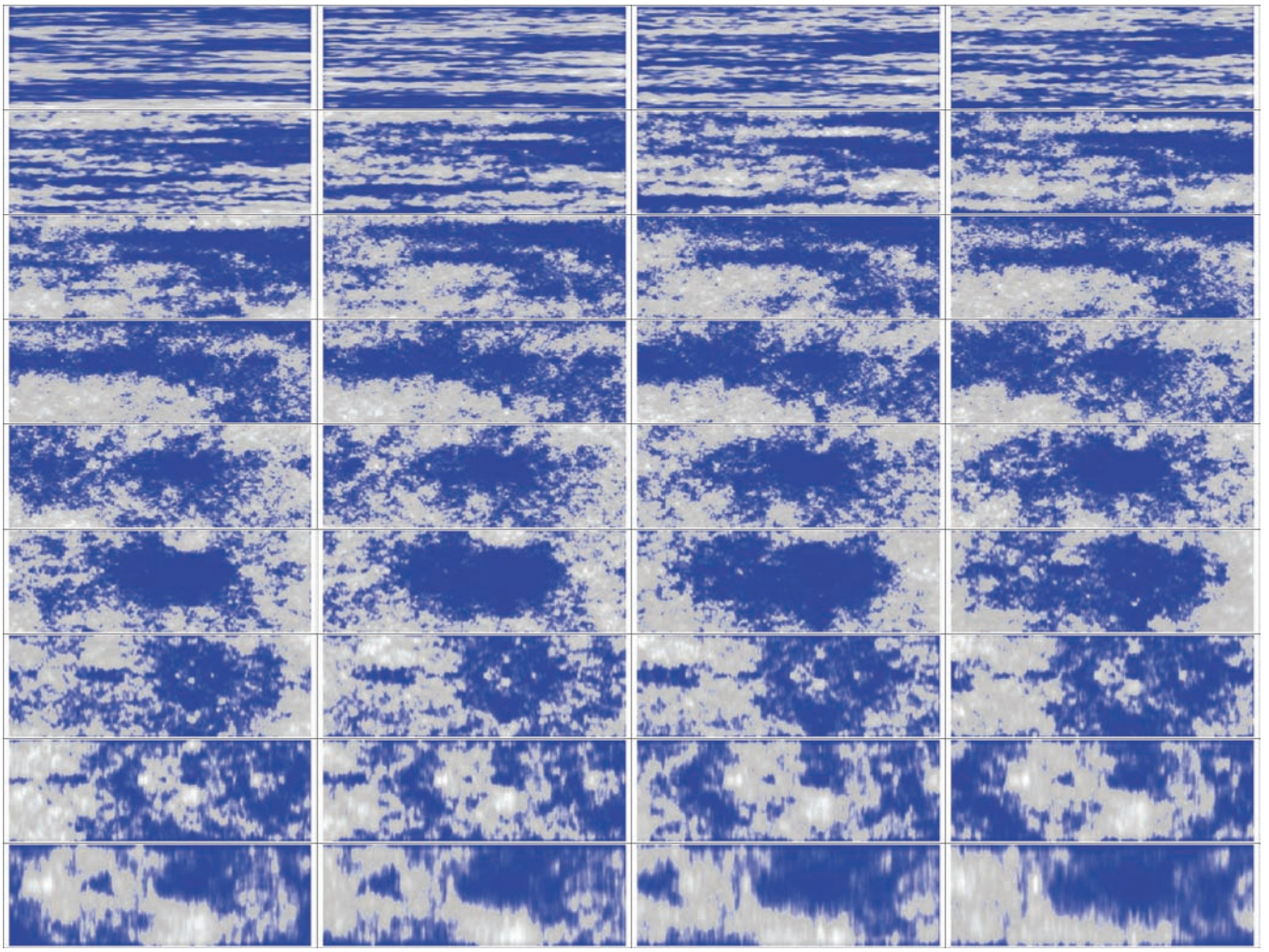

Fig. 21. A sequence from a zoom of a stratified universal multifactal cloud model with $\alpha = 1.8, C_1 = 0.1, H = 1/3, H_z = 5/9$. (From top left to bottom right) Each represents a blow-up by a factor 1.31 (total blow-up is a factor $\approx 24\,000$ from beginning to end). If the top left simulation is an atmospheric cross-section 8 km left to right, 4 km thick, then the final (lower left) image is about 32 cm wide by 16 cm high; the sphero-scale is 1 m as can be roughly visually confirmed since the left-right extent of the simulation second from bottom on the right is 1.02 m where structures can be seen to be roughly roundish. From [Lovejoy & Schertzer, 2010].

reasons discussed below, G is parametrized in the following way:

$$G = \begin{pmatrix} d+c & f-e \\ f+e & d-c \end{pmatrix}; \quad a^2 = c^2 + f^2 - e^2. \tag{79}$$

All the simulations have $\alpha = 1.8, C_1 = 0.1, H = 0.33$ (the empirical parameters for clouds), and are simulated on 256×256 grids with the same starting seed so that the differences are only due to the anisotropy (the colors go from blue to white indicating values low to high). However, there are much more general properties. For instance, the Jacobian of any contraction is T_λ:

$$\det(T_\lambda) = \lambda^{-D_{\rm el}} \tag{80}$$

with:

$$D_{\rm el} = \mathrm{Tr}(G) \tag{81}$$

which corresponds to an effective dimension called "elliptical dimension" in reference to the elliptic-like shape of the balls under a GSI contraction. It is merely the topological dimension $d = \mathrm{Tr}(1)$ of the vector space for the isotropic contraction. On the other hand, differentiation of the "integral" property of linearity with the contraction parameter [Eq. (67)] yields:

$$\lambda \frac{d}{d\lambda} \|\underline{x}_\lambda\| = \nabla_{\underline{x}} \|\underline{x}_\lambda\| \cdot G \cdot \underline{x}_\lambda \tag{82}$$

which rather corresponds to a generalization of Euler's theorem for homogeneous function (obtained for a self-affine G). This differential form

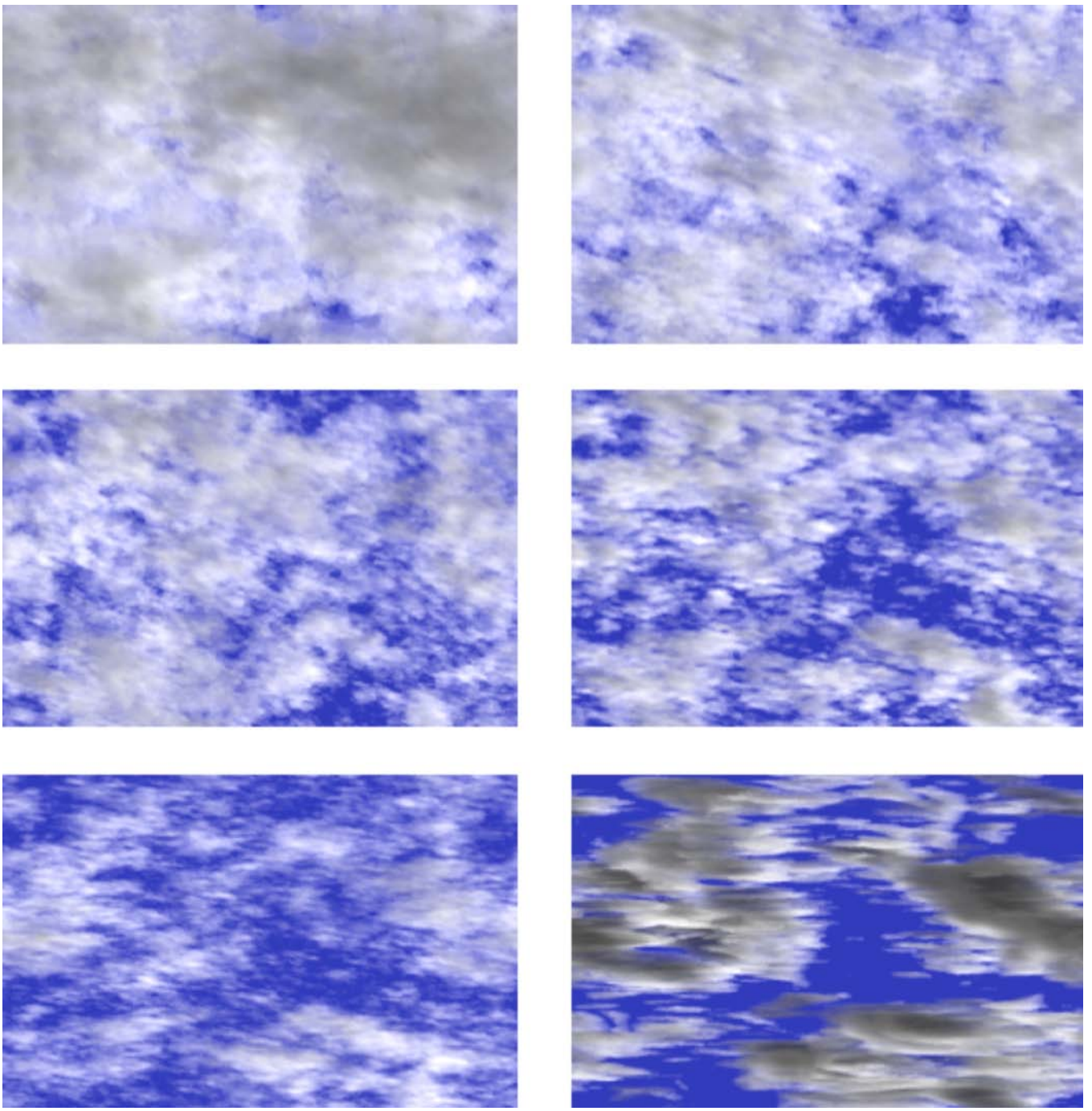

Fig. 22. The effect of the sphero-scale, Cloud parameters: $\alpha = 1.8, C_1 = 0.1, H = 1/3$, r = vertical/horizontal aspect ratio top to bottom: $r = 1/4$, 1, 4, left to right, sphero-scale = 1, 8. From [Lovejoy & Schertzer, 2010].

can be used to assure that balls are strictly decreasing with the contraction T_λ. This can be achieved for:

$$B_L = \{\underline{x} \,|\, (\underline{x}, A\underline{x})^{1/2} \leq L\} \tag{83}$$

where A is a given bilinear application, Eq. (82) indeed yields [Schertzer & Lovejoy, 1985a; Schertzer *et al.*, 1999] the following necessary and sufficient condition that the balls $T_\lambda(B_L) \equiv B_{L/\lambda}$ are strictly decreasing with the contraction group T_λ:

$$\text{Spec}(\text{sym}(AG)) > 0 \tag{84}$$

where $\text{sym}(\cdot)$ denotes the symmetric part of a linear application. When A is furthermore positive and symmetric, i.e. the ball B_L is an ellipsoid, this condition [Eq. (84)] reduces to:

$$\text{Spec}(\text{sym}(G)) > 0 \Leftrightarrow \text{Re}(\text{Spec}(G)) > 0. \tag{85}$$

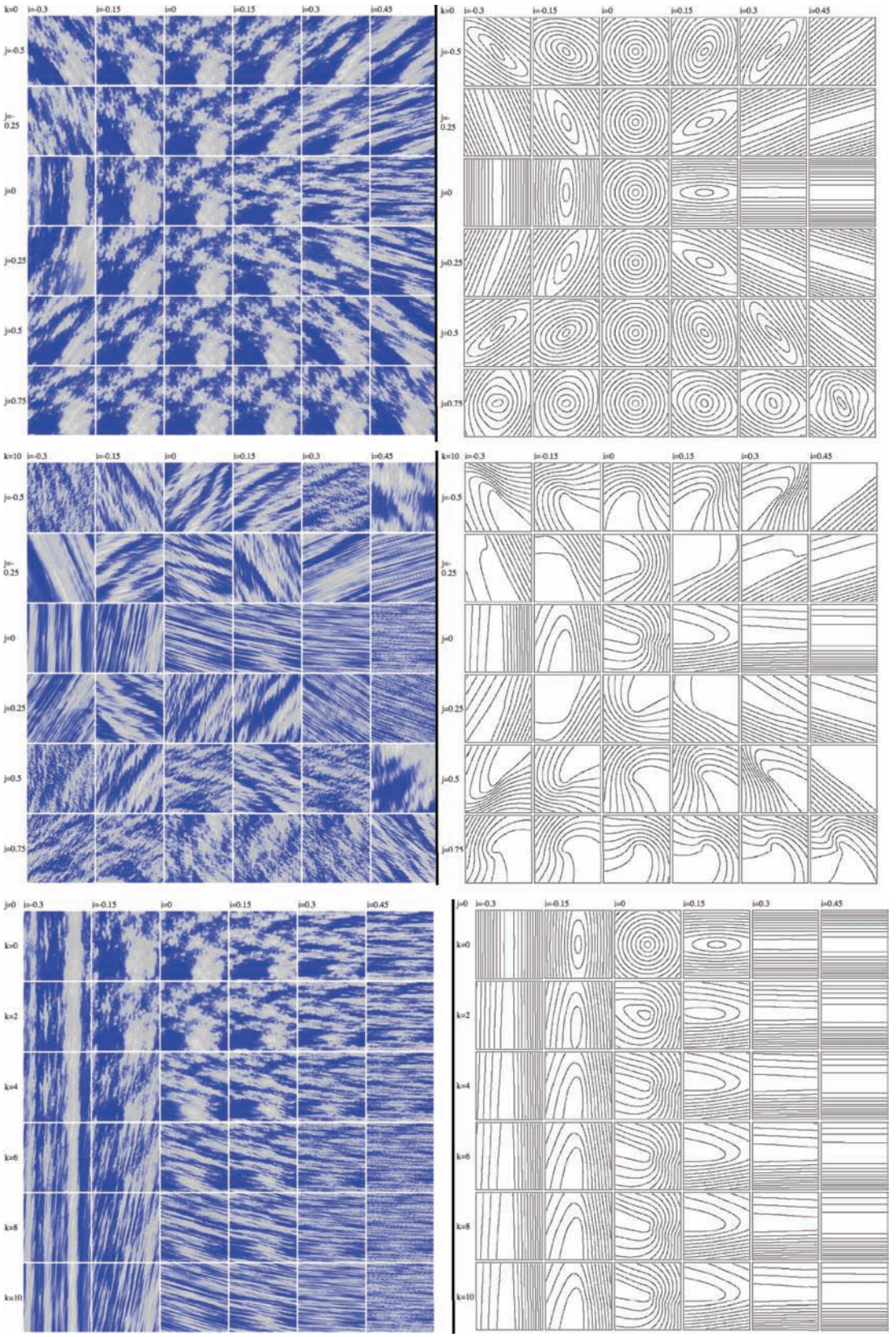

Fig. 23. (Top row) $k = 0$, we vary c (denoted i) from $-0.3, -0.15, \ldots, 0.45$ left to right and e (denoted j) from $-0.5, -0.25, \ldots, 0.75$ top to bottom. On the right we show the contours of the corresponding scale functions. (Middle row) Same except that $k = 10$. (Bottom row) $e = 0$ the c is increased from $-0.3, -0.15, \ldots, 0.45$ left to right, from top to bottom, k is increased from $0, 2, 4, \ldots, 10$. See text for more details. From [Lovejoy & Schertzer, 2007].

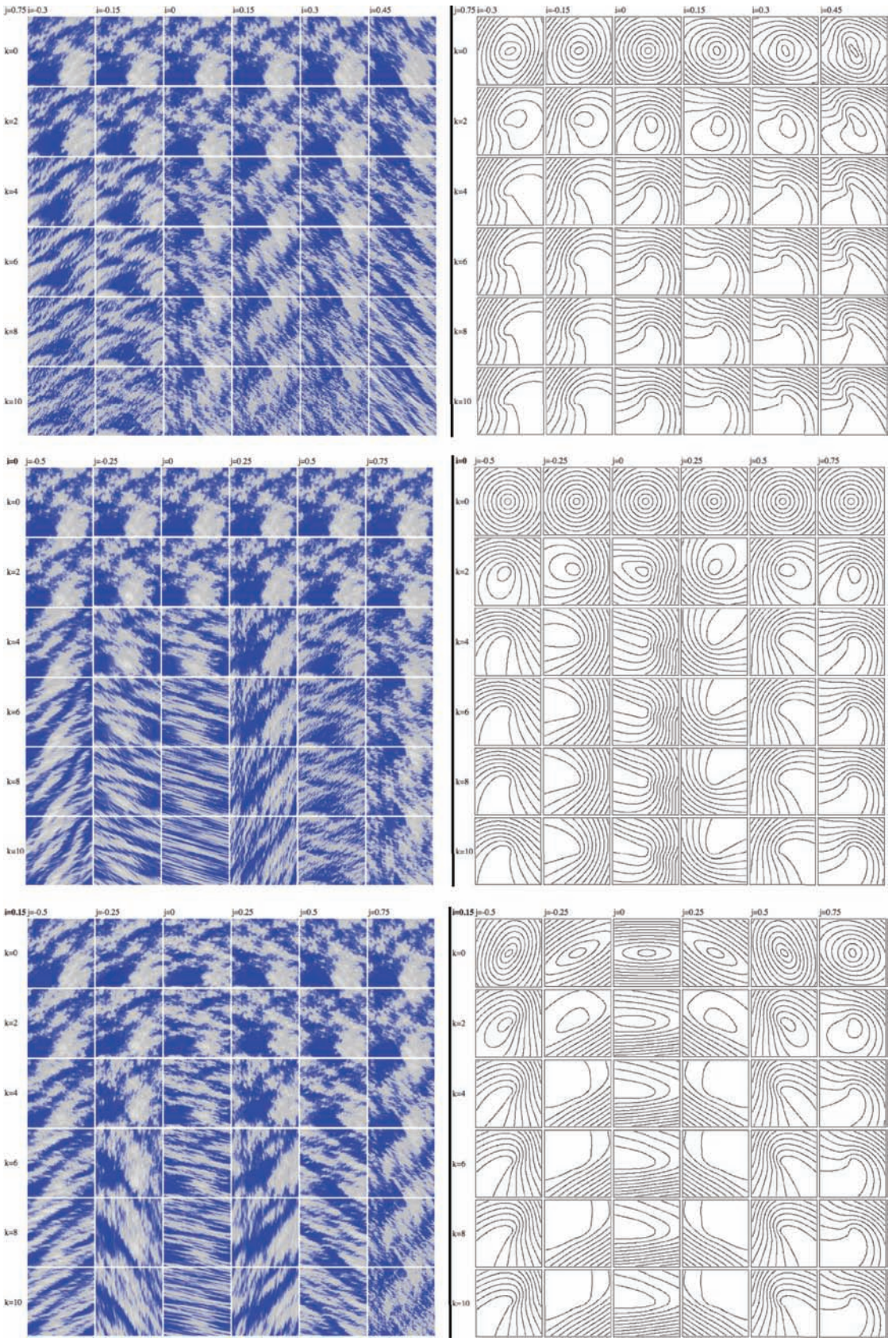

Fig. 24. (Top row) The same as the bottom row of Fig. 23 except that $e = 0.75$. (Middle row) $c = 0$ and e left to right is: $-0.5, -0.25, \ldots, 0.75$. (Bottom row): Same as the middle row except that $c = 0.15$. In all rows, from top to bottom, k is increased $(0, 2, 4, \ldots, 10)$, the right hand shows the corresponding scale functions. From [Lovejoy & Schertzer, 2007].

For the two-dimensional case [and parametrization given by Eq. (79)], this reduces to the following:

$$\begin{aligned} &\mathrm{Tr}(G) > 0 \quad \text{and} \\ &\det(G) > 0 \Leftrightarrow d > 0 \quad \text{and} \quad d^2 > a^2. \end{aligned} \tag{86}$$

8.3. *Nonlinear GSI and Lie cascades*

We will use the example of the two-dimensional generator G with its above parametrization [Eq. (79)] that corresponds to a "pseudo-quaternions" representation:

$$\begin{aligned} G &= d\mathbf{1} + e\mathbf{I} + f\mathbf{J} + c\mathbf{K}; \\ \mathbf{1} &= \begin{bmatrix} 1 & 0 \\ 0 & 1 \end{bmatrix}, \quad \mathbf{I} = \begin{bmatrix} 0 & -1 \\ 1 & 0 \end{bmatrix}, \\ \mathbf{J} &= \begin{bmatrix} 0 & 1 \\ 1 & 0 \end{bmatrix}, \quad \mathbf{K} = \begin{bmatrix} 1 & 0 \\ 0 & -1 \end{bmatrix} \end{aligned} \tag{87}$$

to point out that in a rather general manner linear GSI results can be extended, albeit given technical difficulties briefly mentioned below, to the nonlinear GSI and lead to the general notion of Lie cascades. Let us first point out that there are at least two reasons to look for nonlinear GSI. The first one is that one has often to work with manifolds rather than with vector spaces, the second one [Schertzer & Lovejoy, 1991], not necessarily independent of the previous one, is that one has often to deal with local symmetries, e.g. the original (Weyl's) local gauge invariance, rather than with global ones. The main point is that the generators of the (local) symmetries define Lie algebra whose structure is essential to understand the interrelations between various symmetries.

Indeed, let us consider that the symmetries T_λ and $\tilde{T}_\lambda$, therefore the whole scale symmetry S_λ [Eq. (40)], together with all other potential symmetries (e.g. more classical symmetries such as rotations) smoothly vary with respect to their parameters. These symmetries not only form a group with respect to their composition, but also a smooth manifold and therefore a Lie group G (e.g. [Sattinger & Weaver, 1986]). In a rather general manner, this group is generated from the symmetries that are infinitesimally close to the identity (for infinitesimally small parameter variation), which spans the tangent space to the identity transformation. In fact, these generators form a Lie algebra g, i.e. a vector space with a (bilinear) skewed product called the Lie bracket $[\cdot,\cdot]$ that furthermore satisfies the Jacobi identity. For matrices, the Lie bracket is defined to be the commutator:

$$\big[X, Y\big] = XY - YX \tag{88}$$

In the example of the two-dimensional generator G we have:

$$2I = \big[J, K\big], \quad 2J = \big[I, K\big], \quad 2K = \big[J, I\big] \tag{89}$$

whereas $\mathbf{1}$ obviously commutes with any element of this Lie algebra $l(2, R)$ of the two-dimensional real matrices. Recall that any Lie algebra g is said to be *abelian* if its bracket, whatever is its expression, vanishes (i.e. $\forall X, Y \in g : [X, Y] = 0$, in short: $[g, g] = 0$), a Lie *subalgebra* s of g is a subspace of g that is closed under the Lie bracket (i.e. $[s, s] \subset s$), a subspace l of g is an *ideal* of g if s is not only closed with itself but with g (i.e. $[g, l] \subset l$), the largest abelian ideal of g is called its *radical* and if it is zero g is called semi-simple. The crucial importance of abelian (sub-)algebra is due to the fact that the corresponding Lie (sub-)groups are indeed commutative, i.e. the symmetries commute.

With the help of these definitions, it is rather straightforward to check that the one-dimensional subalgebra R generated by $\mathbf{1}$ is the radical of $l(2, R)$, whereas s spanned by $\{\mathbf{I}, \mathbf{J}, \mathbf{K}\}$ is semi-simple. The latter is classically known as $sl(2, R)$, the special two-dimensional real linear algebra of matrices with zero trace. We have:

$$l(2, R) = R \oplus sl(2, R) \tag{90}$$

which is merely a particular example of the Levi decomposition of any Lie algebra into its radical and a semi-simple subalgebra. It is also important to note that the three two-dimensional subalgebra s_i $(i = 1, 3)$ spanned respectively by $\{\mathbf{1}, \mathbf{I}\}$, $\{\mathbf{1}, \mathbf{J}\}$, $\{\mathbf{1}, \mathbf{K}\}$ are all abelian (s_1 is merely equivalent to the set of complex numbers), but they are not ideals of $l(2, R)$. It means that the corresponding subgroups are commutative, but do not commute with any element of the full group generated by $l(2, R)$. A simple consequence is that if the generator G of T_λ (resp. $\tilde{G}$ of $\tilde{T}_\lambda$) belongs to s_3, then it will commute with any symmetry generated by $\mathbf{K}$, but not with those generated by $\mathbf{I}$, i.e. rotations.

Whereas the mapping from Lie groups to Lie algebra is rather one-to-one, the inverse is often more complex: different Lie groups may have the same Lie algebra. Nevertheless, the exponential map allows to fully capture the local structure of the group from its algebra. Here, the exponential map

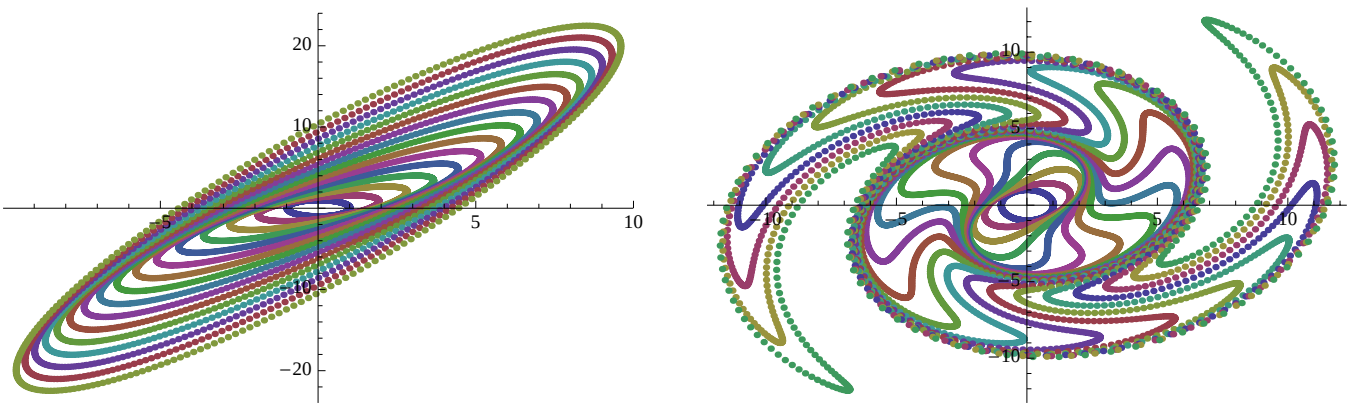

(a) (b)

Fig. 25. GSI balls for $\lambda = 1$ to 10 by steps $\delta\lambda = 0.5$: (a) linear case for $g(\underline{x}) = G\underline{x}$ [Eq. (91)] where the matrix is defined according to Eq. (79) with the set of parameters $(d, c, f, e) = (1, 0.5, 0.5, 1)$, i.e. stratification being dominant, (b) nonlinear case: the parameter e now depends on the location $\underline{x} : e(\underline{x}) = |\underline{x}|^{3/4}$. This introduces an extreme differential rotation.

from a tangent space to its manifold correspond to the generalization of the exponential function, particularly seen under its differential form as:

$$\frac{dx_\lambda}{d\lambda} = -\frac{g(x_\lambda)}{\lambda}. \tag{91}$$

Loosely speaking, one has only to carefully distinguish the tangent space from its manifold, whereas both are confused in the (linear) case of vector spaces. The above mentioned limitation to the local structure is that the integration can introduce an external outer scale, i.e. the inverse of $T_\lambda = T_{1/\lambda}$, i.e. a dilation, for large λ is not always defined.

As simple examples, we can consider the integration of the nonlinear differential equation (91), with the initial condition x_1 belonging to a given ball B_L, still on a vector space E, but where g is nonlinear. Its gradient $\nabla_x g$ is equivalent to a local (infinitesimal) generator G. Therefore, the condition of (local) growth of the balls for linear GSI applies now to $\nabla_x g$. For the two-dimensional case, the same parametrization as before for G [Eq. (87)] corresponds to spatially variable coefficients (d, c, e, f) and if B_L is a symmetric ellipsoid, $\nabla_x g$ needs only to satisfy the same condition [Eq. (86)] as G.

Figure 25(b) is one among many figures that can be obtained in this nonlinear manner. Note due to nonlinearity the balls B_λ, are no longer convex sets, contrary to the linear case.

8.4. *GSI, scaling analysis and differential systems*

GSI has a huge potential of applications when dealing with anisotropy and classical differential systems. Indeed, the classical manner to deal with such problems was to first proceed to a scale analysis, i.e. to define so-called characteristic quantities that help to select a few corresponding relevant terms that will be retained to build up approximations of the original equations. However, as discussed by analysis [Schertzer *et al.*, 2012], on the particular example of the quasi-geostrophic approximation [Charney, 1948], there are many reasons to expect that the scaling of the approximation will be different from the original equations. GSI allows to proceed in a different manner: an anisotropic analysis enables us to select the relevant interactions that occur on a wide range of scales (contrary to the scale analysis, which is local in scale) and obtain a new set of equations, which corresponds to a statistical breaking of an isotropic statistical symmetry, which can be seen as a broad generalization of the spontaneous symmetry breaking. Here, the anisotropic scaling splits a vector equation that admits isotropic scaling into separated component equations. In the case of the vorticity equation this can be obtained by first decomposing the fields and operators into horizontal and vertical components (with respective indices h and v), e.g. for the velocity field u and gradient operator ∇:

$$\underline{u} = \underline{u}_h + \underline{u}_v; \quad \nabla = \nabla_h + \nabla_v \tag{92}$$

and with the help of the following pushback transforms [Schertzer *et al.*, 2012]:

$$\begin{aligned} T^*_\lambda(\underline{u}) &= \lambda^\gamma(\underline{u}_h + \lambda^h \underline{u}_v); \\ T^*_\lambda(\nabla) &= \lambda^\gamma(\nabla_h + \lambda^{-h}\nabla_v) \end{aligned} \tag{93}$$

where h is the scaling anisotropy exponent of the vertical vs. the horizontal, as well as the corresponding decomposition of the vorticity ω into:

$$\begin{aligned} \underline{\omega} = \underline{\omega}_v + \underline{\sigma} + \underline{\tau}; \quad \underline{\omega}_v = \nabla_h \times \underline{u}_h, \\ \underline{\sigma} = \nabla_h \times \underline{u}_v, \quad \underline{\tau} = \nabla_v \times \underline{u}_h \end{aligned} \tag{94}$$

where $\underline{\omega}_h = \underline{\sigma}+\underline{\tau}$ is the horizontal vorticity, which is assumed to be negligible at large scales where the (almost vertical) Earth rotation $\underline{\Omega}$ is assumed to be dominant. A careful examination of the scaling exponents resulting from Eq. (93) involved in the vorticity equation ($D./Dt$ denotes the Lagrangian time derivative):

$$\frac{D\underline{\omega}}{Dt} = \underline{\omega} \cdot \nabla \underline{u} \tag{95}$$

points out that the latter splits into the three following equations:

$$\begin{aligned} \frac{D\underline{\sigma}}{Dt} &= \underline{\sigma} \cdot \nabla_h \underline{u}_h \\ \frac{D\underline{\tau}}{Dt} &= (\underline{\tau} \cdot \nabla_h + \underline{\omega}_v \cdot \nabla_v)\underline{u}_h \\ \frac{D\underline{\omega}_v}{Dt} &= (\underline{\tau} \cdot \nabla_h + \underline{\omega}_v \cdot \nabla_v)\underline{u}_v \end{aligned} \tag{96}$$

Conversely, these three equations, together with the large scale condition $\underline{\omega}_v \approx \underline{\Omega}$, allow an anisotropic scaling like that displayed by Eq. (93), as well as a nonlinear growth of the horizontal vorticity. The latter mechanism is absent from the quasi-geostrophic approximation, which corresponds to $\underline{\sigma} \equiv \underline{\tau} \equiv \underline{0}$ and the approximation:

$$\frac{D\underline{\omega}_v}{Dt} \approx \underline{\Omega}_v \cdot \nabla_v \underline{u}_v. \tag{97}$$

Contrary to the quasi-geostrophic equations, the fractional vorticity equations (96) are not an approximation of the vorticity equations (95), because solutions of the former are also solutions of the latter. They rather correspond to select relevant interactions to provide solutions having a scaling as prescribed by Eq. (93). This explains the extreme contrast between Eq. (96) with a 3D nonlinear vorticity stretching and Eq. (96) with only a weak, linear stretching. We believe that this scaling analysis is rather illustrative of the potential of GSI to better investigate the nonlinear generating equations of anisotropic scaling fields, well beyond the scale analysis and the resulting classical approximations.

9. The Extremes: Self-Organized Criticality and Multifractal Phase Transitions

9.1. *The singular small-scale limit of a cascade process*

The small-scale limit $\lambda \to \infty$ of a cascade process is very singular since for any positive singularity γ, the density $\varepsilon_\lambda \approx \lambda^\gamma$ diverges. These divergences are statistically significant for $\gamma > C_1$, since it corresponds to $q > 1$ and $K(q) > 0$, therefore to $\langle \varepsilon_\lambda \rangle = \lambda^{K(q)} \to \infty$. This singular small-scale divergence means that if a limit exists, it is not in the sense of functions. This is similar to the Dirac δ-"function", in fact the Dirac δ-measure, which is not a function at all but a "generalized function" defined as a limit of functions. The Dirac δ-measure is indeed only meaningful if we integrate over it. It is rather obvious that the β-model corresponds to a (random) generalization of the Dirac δ-measure for points belonging to a fractal set of codimension $c = D - D_s$. Conversely, the Dirac δ-measure can be understood as the particular (deterministic) case corresponding to a codimension $c = D$ and dimension $D_s = 0$, i.e. to isolated points.

As a consequence, one has to consider the limit of the corresponding measures $\Pi_\lambda(A) \to \Pi_\infty(A)$ over compact sets A of dimension D, i.e. the D-dimensional integration of the density ε_λ over A:

$$\Pi_\infty(A) = \lim_{\lambda \to \infty} \Pi_\lambda(A) = \lim_{\lambda \to \infty} \int_A \varepsilon_\lambda d^D \underline{x}. \tag{98}$$

In agreement with turbulent nomenclature, the integral Π_λ can be termed a "flux" (of energy) through the scale $l = L/\lambda$, whereas ε_λ can be called (energy) flux density at this scale. Therefore, we anticipate that the fluxes (but not the densities) converge as $\lambda \to \infty$. Still due to the singular nature of the limit, we may expect that convergence can only occur over a limited range of order q of the statistical moments:

$$\exists\, q_D > 1, \quad \forall\, q \geq q_D : \langle \Pi_\infty(A)^q \rangle = \infty \tag{99}$$

whereas:

$$\forall\, \lambda < \infty : \langle \Pi_\lambda(A)^q \rangle < \infty. \tag{100}$$

The subscript D of the critical order q underscores its dependence on the dimension of the space over which it is integrated. This dependence can be used [Schertzer & Lovejoy, 1984] to demonstrate that cascade processes are generically multifractals: the dependence of q_D on D defines a hierarchy of

fractal sets. An important consequence of the divergence of moments [Eq. (99)] is also the exponent of the power-law fall-off of the probability distribution:

$$\exists\, q_D > 1, \quad \pi \gg 1 : \Pr(\Pi_\infty(A) > \pi) \approx \pi^{-q_D}. \tag{101}$$

Equations (99)–(101) are equivalent and the divergence of moments has many practical implications that we discuss below. The divergence of moments coupled with fractal structures is often considered the hallmark of self-organized criticality (SOC; [Bak *et al.*, 1987, 1988]) so that cascade processes can be considered a nonclassical route to SOC. In this respect, we could note an important difference: classical SOC is a cellular-automaton model (the prototype being the "sandpile" and its avalanches) that requires a "zero-flux" limit: in the sandpile each grain must be added one at a time only after the activity induced by the previous grain is over. In contrast, the cascades require a quasi-constant flux, and this is generally more physical.

To graphically appreciate the propensity for multifractal processes to generate extremes at all scales, see Fig. 26. In order to make the point that occasionally very rare events occur, a single value (the maximum) of the subgenerator was boosted by a factor N (placed at the centre of the simulation).

9.2. *Bare and dressed cascades*

The singular limit of the cascade process requires us to distinguish between the properties of a cascade stopped at a finite resolution λ, (all of whose positive moments are finite) from those corresponding to integrals (at the same scale) of the process taken to the small scale limit. Schertzer and Lovejoy [1987] argued that physically this difference is due to the effect of the small scale interactions, which "dress" the former "bare" process. This is reminiscent of what happens in renormalization when higher and higher order interactions are taken into account. In the same way, we distinguish between the "bare" cascade quantities obtained after the cascade has proceeded down to a finite resolution λ, and the corresponding "dressed" quantity obtained after integrating a completed cascade over the same scale ($l = L/\lambda$; see Fig. 11 for an illustration of a finite resolution Λ). Due to the group property of a multiplicative cascade discussed in Sec. 5, a dressed cascade factors into its bare part and the hidden part, which corresponds to a flux of a cascade from L to $L\lambda/\Lambda$ rescaled with the help of the pushback operator $T^*_\lambda\lambda$. For small enough order moments, the flux prefactor remains finite in the limit $\Lambda \to \infty$, the bare and dressed scaling properties are the same. However for $q \geq q_D$ this prefactor begins to scale with Λ/λ, so that a drastic change occurs; it diverges with Λ.

In a real system, the scaling is cutoff by dissipation so that while the moments $q < q_D$ depend on the large scales in contrast, the value of the moments $q > q_D$ will depend on the small scale details. Since it is this small scale activity that causes the divergence, in analogy with the classical (chaotic) metaphor for sensitive dependence, this has been called the "multifractal butterfly effect" [Lovejoy & Schertzer, 1998].

9.3. *Scale dependence and divergence of the flux: The heuristic argument*

Let us first consider some simple heuristics whose main interest is that they are model independent. They are based on the fact that a D-dimensional integration of a singularity γ just corresponds to shifting the latter by $-D$, which corresponds to the scaling exponent of the elementary volume of integration. As a consequence, all singularities of order $\gamma < D$ will be smoothed out. This already explains why the question of statistical divergences is beyond the scope of deterministic multifractal formalisms (see Sec. 4.3). On the contrary, divergences arising from $\gamma \geq D$ will not be smoothed out and therefore the scale of observation is irrelevant: the flux will scale with the inner scale of activity of the cascade and therefore will diverge as $\Lambda \to \infty$. However due to its low statistical weight, this divergence may remain statistically insignificant. Nevertheless, one may reach a critical $\gamma_D \geq D$ where it becomes significant. Above γ_D, the observed dressed codimension function $c_d(\gamma)$ no longer corresponds to $c(\gamma)$: the dressed quantities will have much larger fluctuations than the bare quantities. $c_d(\gamma)$ can therefore be estimated by considering that it should maximize the occurrences of high singularities, while nevertheless respecting the convexity constraint. This means that $c_d(\gamma)$ should follow the tangency of $c(\gamma)$ at γ_D:

$$\begin{aligned} \gamma \leq \gamma_D &: c_d(\gamma) = c(\gamma) \\ \gamma \geq \gamma_D &: c_d(\gamma) = c(\gamma_D) + q_D(\gamma - \gamma_D) \end{aligned} \tag{102}$$

Since $q_D = c'(\gamma_D)$ is the critical order corresponding to γ_D in the framework of the Legendre

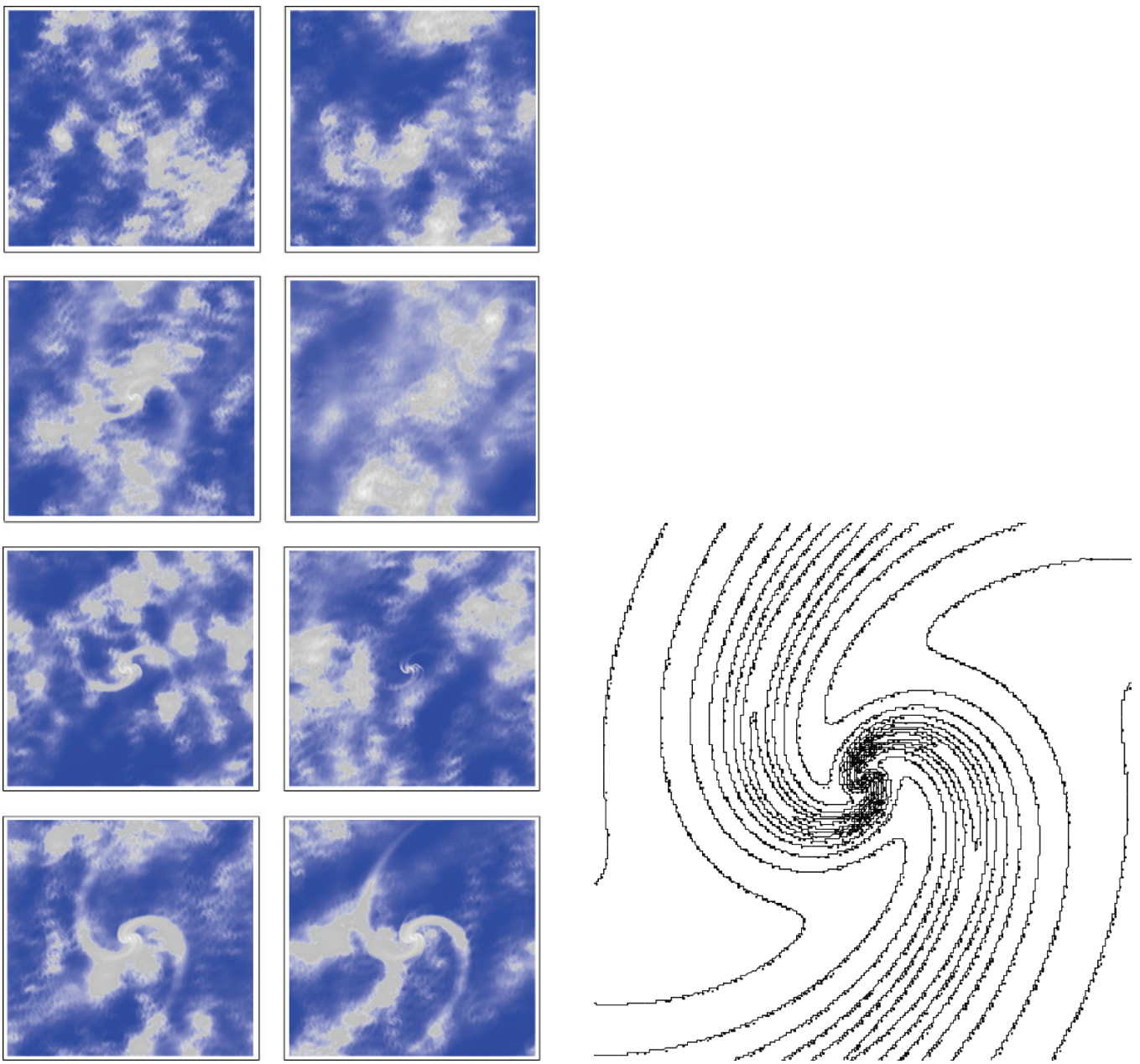

(a) (b)

Fig. 26. This shows two realizations (a) of a random multifractal process with a single value of the maximum of the subgenerator (at the centre of a 512×512 grid) boosted by factors of N from 16 to 64 (increasing by $2^{(1/2)}$ from top to bottom) in order to simulate very rare events. The scaling is anisotropic with complex eigenvalues of G, the scale function is shown in (b).

duality (Sec. 4.2), we see that the divergence of the statistical moments for $q \geq q_D$ is a consequence of the fact that a straight line is singular for the Legendre transform. We therefore obtain:

$$q < q_D: \quad K_d(q) = K(q); \quad q \geq q_D: \quad K_d(q) = \infty \tag{103}$$

$$\begin{aligned} K_d(q) &= K(q); \quad q < q_D \\ K_d(q) &= \infty; \quad q \geq q_D. \end{aligned} \tag{104}$$

This heuristic argument can be made rigorous by introducing [Schertzer & Lovejoy, 1987] the Trace Moments of the flux which are simpler to handle than the statistical moments of the flux.

9.4. *Finite sample size effects*

In practice, we are only able to examine finite samples, hence instead of computing the theoretical

moments:

$$\langle X^q \rangle = \int x^q dP_X \tag{105}$$

we only deal with estimates, the most usual ones being an average over the N_s independent samples:

$$\{X^q\}_s = \frac{1}{N_s} \sum_{i=1}^{N_s} X_i^q. \tag{106}$$

As long as the law of large numbers applies, these estimates converge towards the theoretical moments:

$$\langle X^q \rangle = \lim_{N_s \to \infty} \{X^q\}_s. \tag{107}$$

One may also consider space/time averages and ergodicity assumptions. In our case, we must consider a combination of statistical and space/time averaging. A first consequence of finite N_s is that only a limited range of q's can in fact be safely explored: as we now show, estimates of moments of higher order give no real information about the process and may lead to erroneous interpretations, e.g. there had been speculations on the significance of the $q \to \infty$ limit on the basis of finite empirical samples of turbulence data.

The limits imposed by finite sample sizes can best be understood with the help of the sampling dimension D_s [Eq. (19) and Sec. 4.1]. As we increase D_s (i.e. the number N_s of samples), we gradually explore the entire probability space encountering extreme but rare events that would almost surely be missed on any finite sample (Fig. 27), i.e. larger and larger sampling singularity γ_s [Eq. (19) and Fig. 8(b) for illustration].

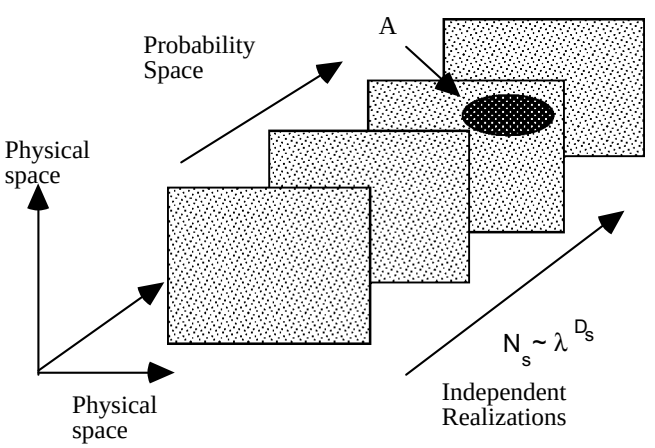

Fig. 27. Illustration showing how in random processes the effective dimension of space (D) can be augmented by considering many independent realizations N_s. As $N_s \to \infty$, the entire (infinite dimensional) probability space is more and more explored. From [Schertzer & Lovejoy, 1993].

The Legendre transform of $c_s(\gamma) = c(\gamma_s)$ with $\gamma \geq \gamma_s$ leads to a spurious linear estimate K_s instead of the nonlinear K for $q > q_s$ where $q_s = c'(\gamma_s)$ is the maximum moment that can accurately be estimated:

$$\begin{gathered} q \geq q_s : K_s(q) = \gamma_s(q - q_s) + K(q_s); \\ q < q_s; \quad K_s(q) = K(q). \end{gathered} \tag{108}$$

In Sec. 9.5.2 we show that this linear behavior corresponds to the multifractal analogue of a second order phase transition and therefore is rather model-independent.

9.5. *Multifractal phase transitions*

9.5.1. *Flux dynamics and thermodynamics*

As discussed by various authors [Schuster, 1988; Tel, 1988; Schertzer & Lovejoy, 1992, 1994; Schertzer *et al.*, 1993], there are formal analogies between multifractal exponents and standard thermodynamic variables. However, depending on the multifractal framework there are notable differences of appreciation. For the codimension multifractal formalism, Table 1 displays the analogues between what can be called (statistical) "fluxdynamics" [Schertzer & Lovejoy, 1991] and classical thermodynamics. The expression "flux dynamics" comes from the fact that the main quantity of interest is the energy flux for systems out of equilibrium instead of the energy for systems in thermodynamic equilibrium. Since the analogies are based on the exponents of the probability and number densities these analogues are more easily and naturally obtained in the codimension framework, which define respectively the codimension $c(\gamma)$ of a singularity γ and the $D - S(E)$ entropy of a state energy E. The Legendre conjugate variables of the singularity and the energy are respectively the moment of order q and the (reciprocal) temperature $\beta = 1/T$. Similarly, the scaling moment function $K(q)$ is the analogue of a (Massieu) potential (= the free energy/T).

Discontinuities in the analogues of the free energy (the dual codimension function $C(q) = K(q)/(q-1)$) and the thermodynamic potential ($K(q)$) correspond to multifractal phase transitions (see Fig. 28 for illustrations). However, thermodynamics applies to systems in equilibrium and without dissipation, whereas flux dynamics applies to systems far from thermodynamic equilibrium which are strongly dissipative. A practical consequence is

Table 1. Correspondence between fluxdynamics and thermodynamics (setting for notation simplicity $k_B = 1$ for the Boltzman's constant k_B): $\Sigma(\beta)$ being the Massieu potential, $F(\beta)$ the Helmhotz free energy. From [Schertzer & Lovejoy, 1993].

Flux Dynamics	Thermodynamics
Probability space	Phase space
Moment order: q	(Reciprocal) Temperature: $\beta = T^{-1}$
Singularity order: γ	(Negative) Energy: $-E$
Generator	(Negative) Hamiltonian
Singularity codimension: $c(\gamma)$	Codimension of entropy: $D - S(E)$
Scaling moment function: $K(q) = \max_{\gamma}(q\gamma - c(\gamma))$	(Negative) Massieu potential: $-\Sigma(\beta) = -\min_{E}(\beta E - S(E))$
Dual codimension function: $C(q) = K(q)/(q-1)$	(Negative) Free energy $-F(\beta) = -\Sigma(\beta)/\beta$
Dimension of integration: D	External field: h
Ratio of scales: λ	Correlation length: ξ

that in order to define its statistics, a multifractal process fundamentally requires an infinite hierarchy of temperatures, rather than a single temperature. Therefore *observing* (i.e. with a finite N_s, D_s) a multifractal process at a given temperature (i.e. q) only gives very limited information about the process. Similarly, a multifractal phase transition is associated with a qualitative change of *observation* of the *same* system when one changes the observation temperature (i.e. changes q), whereas a thermodynamic phase transition corresponds to a qualitative change of the *behavior* of the system under observation.

9.5.2. *Second order phase transition*

Finite sample size effects (Sec. 9.4) can be now understood as corresponding to a phase transition of second order and in fact a "frozen free energy" transition which has been discussed in various contexts [Derrida & Gardner, 1986; Mesard *et al.*, 1987; Brax & Pechanski, 1991]. Indeed, we saw that the almost sure highest order singularity (γ_s) which can be observed on N_s realizations, yields with the help of the Legendre transform a linear behavior of the observed K_s [Eq. (108)] for $q > q_s$, whereas it is nonlinear as $K(q)$ for $q < q_s$. Therefore, K_s has a discontinuity of second order at γ_s (see Fig. 28 for an illustration). On the other hand, this linear behavior implies that the observed analogue of the free energy $C_s(q)$ seems to be "frozen" for low temperature ($q \to \infty$), since we have:

$$C_s(q) \equiv \frac{K_s(q)}{q-1} \approx \gamma_s \left(1 + q^{-1}\left(\frac{1-q_s}{\gamma_s}\right)\right). \quad (109)$$

Further to the heuristics derivation we have presented here, some exact mathematical results have been obtained, which are however restricted to discrete cascades and furthermore to $D_s = 1$. On the other hand, the notion of second order phase transition is interesting, because it is rather model-independent as it is based on the analogies of the statistical exponents of the cascade. Indeed, it should occur as soon as there are no bounds on the singularities or their range exceeds the critical γ_s.

9.5.3. *First order phase transition*

We can now revisit the question of the divergence of moments (Sec. 9.3) taking care of the sample

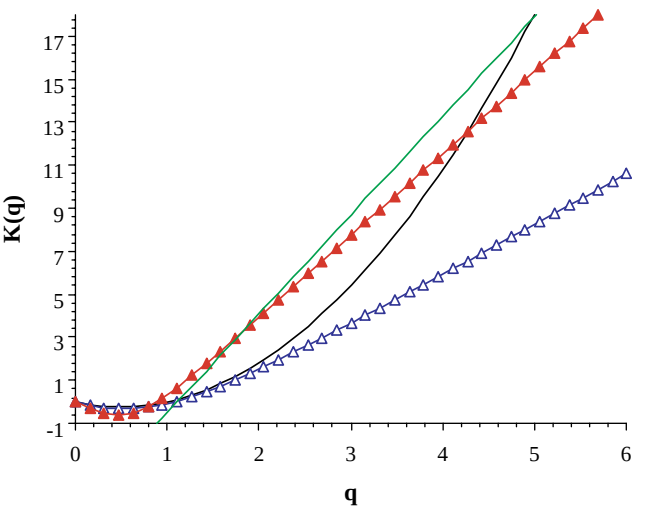

Fig. 28. A numerical simulation of multifractal phase transitions for a universal multifractal ($\alpha = 2, C_1 = 0.9, \Lambda = 2^{10}$, 2^9 realizations): $K(q)$ (theoretical, parabola), $K_s(q)$ (observed second order transition — along a tangency to $K(q)$ for large q's — corresponding to the finite size of the sample at the highest resolution, bare, open triangles), $K_{d,s}(q)$ (observed first order transition, partially dressed ($\lambda = 2^7$) above $K(q)$ for large q's, closed triangles), $K_{d,s}(q)$ (theoretical first order transition, fully dressed, straight line). Reproduced from [Schertzer *et al.*, 1993].

size finite effects, in the heuristic and very general framework we discussed in Sec. 4. We pointed out that above a critical singularity γ_D, the dressed codimension $c_d(\gamma)$ becomes linear [Eq. (102)]. Due to the definition of the codimension [Eq. (16)], this corresponds to a power-law for the probability distribution [Eq. (101)], and by consequence to a divergence of statistical moments [Eq. (99)]. However, due to the finite size of the samples, one obviously cannot observe with the help of the statistical moment estimates this divergence, but in fact only a first order transition, instead of the second order transition discussed above (Sec. 9.5.2). Indeed, following the argument for Eq. (19), the maximum observable dressed singularity $\gamma_{d,s}$ is the solution of:

$$c_d(\gamma_{d,s}) = \Delta_s. \tag{110}$$

By taking the Legendre transform of c_d with the restriction $\gamma_d \leq \gamma_{d,s}$, we no longer obtain the theoretical $K_d(q) = \infty$ for $q > q_D$ [Eq. (103)], but then obtain the finite sample dressed $K_{d,s}(q)$:

$$\begin{aligned} &q \leq q_D : K_{d,s}(q) = K(q); \\ &q \geq q_D : K_{d,s}(q) = \gamma_{d,s}(q - q_D) + K(q_D). \end{aligned} \tag{111}$$

As expected, Eq. (103) is recovered for $N_s \to \infty$, due to the fact that $\gamma_{d,s} \to \infty$. For N_s large but finite, there will be a high q (low temperature) first order phase transition, whereas the scale breaking mechanism proposed for phase transitions in strange attractors [Szépfalusy *et al.*, 1987; Csordas & Szépfalusy, 1989; Barkley & Cumming, 1990] is fundamentally limited to high or negative temperatures (small or negative q). This transition corresponds to a jump in the first derivative $K'(q)$ of the potential analogue [Schertzer *et al.*, 1993]:

$$\begin{aligned} \Delta K'(q_D) &\equiv K'_{d,s}(q_D) - K'(q_D) \\ &= \gamma_{d,s} - \gamma_D = \frac{\Delta_s - c(\gamma_D)}{q_D}. \end{aligned} \tag{112}$$

On small sample size ($\Delta_s \approx c(\gamma_D)$), this transition will be missed, the free energy simply becomes frozen and we obtain: $K_{d,s}(q) \approx (q-1)D$, which was already discussed with the help of some empirical data [Schertzer & Lovejoy, 1984], whereas Eq. (111) corresponds to an improvement of earlier works on "pseudo scaling" [Schertzer & Lovejoy, 1984, 1987]. The above relations, especially Eq. (112), were tested numerically with the help of lognormal universal multifractals (see Fig. 28), as well on atmospheric data (see Fig. 29).

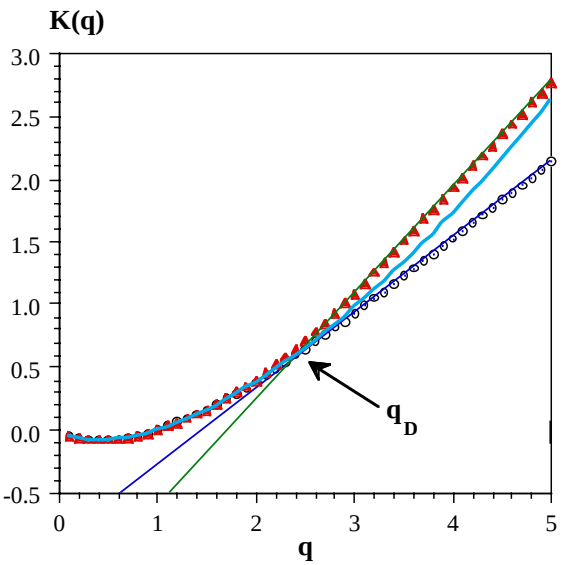

Fig. 29. The empirical scaling exponent moment function $K_{d,s}(q)$ of the atmospheric turbulence energy flux using respectively 4 (crosses) and 704 (dots) 10 Hz time series, compared to the (bare) $K(q)$ (continuous line) with universal multifractal parameters $\alpha = 1.45$ and $C_1 = 0.24$. All these curves collapse together until $q_D \approx 2.4$, whereas for larger moment orders q's the empirical estimates become linear. The curve $K_{d,s}(q)$ corresponding to an average of 704 realizations is clearly above $K_{d,s}(q)$, which is only possible for a first order multifractal transition, whereas a second order transition curve would correspond to a tangent to $K(q)$. Reproduced from [Schmitt *et al.*, 1994].

10. Future Directions

The goal of this paper was to present the main theoretical developments of multifractals and generalized scale invariance during the two and a half decades of their explicit existence, including numerical simulations and data analysis. We hope that it reveals the awesome simplification that multifractals can bring to complex systems by reducing their complexity with the help of a quite diverse and widely applicable scale symmetries.

Although multifractals are increasingly understood as a basic framework for analyzing and simulating extremely variable processes, in many scientific disciplines and in particular in geophysics, there is still a wide gap between their potential and their actual use. Beyond the familiar slow and inhomogeneous pace of the diffusion of scientific knowledge, an additional reason for this could be obstacles inherited from older, preexisting and

highly restrictive concepts of scaling: for example that they are only geometrical descriptors or that they are inherently isotropic. The latter had been a particularly important obstacle for the development of multifractals in geophysics due to privileged directions generated by gravity and the Earth's rotation: a generalization of the scale notion was necessary to overcome it.

We therefore expect that future developments of multifractals will build upon their most recent advances so as to better tackle issues arising in geophysical systems. This should include new advances on model independent characteristics, such as universality classes and multifractal phase transitions (beyond the scalar case), to substantially improving existing statistical estimators of multifractal parameters, as well as their related uncertainties. Another axis concerns the notion of scale itself: the further exploration of possible features of generalized (space-time) scales in particular in dynamical multifractal processes. This raises the questions of multifractal predictability and prediction that we did not address here, although we may expect a rapid development of multifractal forecast techniques, as well as the discovery of stimulating connections with the theory of random dynamical systems. Our current understanding of multifractal extremes points out the necessity — as well as the possibility — of developing a new extreme value theory that could deal with processes having long-range dependencies. At the same time, there remains the fundamental question of establishing a more direct connection, i.e. well beyond the present arguments based on numerics, phenomenology or on a too formal symmetry, between multifractals and the deterministic-like nonlinear equations that are supposed to generate them, in particular the Navier–Stokes equations. We pointed out current developments in this direction. This would have many fundamental consequences such as opening the road to new renormalization techniques able to grasp intermittency as well as to a better knowledge of the mathematical properties of the solutions of these equations.

References

Aitchison, J. & Brown, J. A. C. [1957] *The Lognormal Distribution, with Special Reference to Its Uses in Economics* (Cambridge University Press).

Anselmet, F., Gagne, Y., Hopfinger, E. & Antonia, R. A. [1984] "High-order velocity structure functions in turbulent shear flows," *J. Fluid Mech.* **140**, 63.

Bak, P., Tang, C. & Weiessenfeld, K. [1987] "Self-organized criticality: An explanation of 1/f noise," *Phys. Rev. Lett.* **59**, 381–384.

Bak, P., Tang, C. & Weiessenfeld, K. [1988] "Self-organized criticality," *Phys. Rev. A* **38**, 364–374.

Bak, P. & Tang, C. [1989] "Earthquakes as a self-organized phenomenon," *J. Geophys. Res.* **94**, 635–637.

Barkley, D. & Cumming, A. [1990] "Thermodynamic of the quasiperiodic parameter set at the borderline of chaos: Experimental results," *Phys. Rev. Lett.* **64**, 327.

Bender, C. M. & Orszag, S. A. [1978] *Advanced Mathematical Methods for Scientists and Engineers* (McGraw Hill, NY).

Bendjoudi, H., Hubert, P., Schertzer, D. & Lovejoy, S. [1997] "Interprétation multifractale des courbes intensité-durée-fréquence des précipitations, multifractal point of view on rainfall intensity-duration-frequency curves," *Comptes Rendus de l'Académie des Sciences — Series IIA — Earth and Planetary Science* **325**, 323–326.

Benzi, R., Parisi, G., Sutera, A. & Vulpiani, A. [1982] "Stochastic resonnance in climate change," *Tellus* **34**, 10–15.

Benzi, R. [2010] "Stochastic resonance: From climate to biology," *Nonlin. Process. Geophys.* **17**, 431–441.

Bochner, S. [1955] *Harmonic Analysis and the Theory of Probability* (University of California Press, Berkeley and Los Angeles).

Brax, P. & Pechanski, R. [1991] "Levy stable law description on intermittent behaviour and quark-gluon phase transitions," *Phys. Lett. B* **253**, 225–230.

Buckingham, E. [1914] "Physically similar systems: Illustrations of the use of dimensional equations," *Phys. Rev.* **4**, 345–376.

Buckingham, E. [1915] "The principle of similitude," *Nature* **96**, 396–397.

Charney, J. G. [1948] "On the scale of atmospheric motions," *Geophys. Publ. Oslo* **17**, 1–17.

Chigirinskaya, Y., Schertzer, D., Lovejoy, S., Lazarev, A. & Ordanovich, A. [1994] "Unified multifractal atmospheric dynamics tested in the tropics, Part I: Horizontal scaling and self organized criticality," *Nonlin. Process. Geophys.* **1**, 105–114.

Chigirinskaya, Y. & Schertzer, D. [1996] "Dynamical hierarchical cascade models, multifractal space-time intermittency and lie structure in turbulence," *Stochastic Models in Geosystems*, eds. Woyczynski, W. A. & Molchanov, S. S. (Springer-Verlag, NY).

Csordas, A. & Szépfalusy, P. [1989] "Singularities in Renyi information as phase transition in chaotic states," *Phys. Rev. A* **39**, 4767–4777.

Derrida, B. and Gardner, E. [1986] "Solution of the generalised random energy model," *J. Phys. C* **19**, 2253–2274.

Feller, W. [1971] *An Introduction to Probability Theory and Its Applications*, Vol. 2 (Wiley, NY).

Frisch, U., Sulem, P. L. & Nelkin, M. [1978] "A simple dynamical model of intermittency in fully develop turbulence," *J. Fluid Mech.* **87**, 719–724.

Frisch, U. [1995] *Turbulence*: *The Legacy of A. N. Kolmogorov* (Cambridge University Press, Cambridge).

Gagnon, J. S., Lovejoy, S. & Schertzer, D. [2006] "Multifractal earth topography," *Nonlin. Process. Geophys.* **13**, 541–570.

Gires, A., Tchiguirinskaia, I., Schertzer, D. & Lovejoy, S. [2011] "Multifractal and spatio-temporal analysis of the rainfall output of the méso-nh model and radar data," *Hydrol. Sci. J.* **56**, 380–396.

Gnedenko, B. V. [1943] "Sur la distribution limite du terme maximum d'une série aléatoire," *Ann. Math.* **44**, 423–453.

Gnedenko, B. V. & Kolmogorov, A. N. [1954] *Limit Distribution for Sums of Independent Random Variables* (Addision-Wesley).

Gupta, V. K. & Waymire, E. [1993] "A statistical analysis of mesoscale rainfall as a random cascade," *J. Appl. Meteorol.* **32**, 251–267.

Halsey, T. C., Jensen, M. H., Kadanoff, L. P., Procaccia, I. & Shraiman, B. [1986] "Fractal measures and their singularities: The characterization of strange sets," *Phys. Rev. A* **33**, 1141–1151.

Hentschel, H. G. E. & Procaccia, I. [1983] "The infinite number of generalized dimensions of fractals and strange attractors," *Physica D* **8**, 435–444.

Kahane, J. P. [1985] "Sur le chaos multiplicatif," *Annales des Siences Mathématique du Québec* **9**, 435.

Kapteyn, J. C. [1903] *Skew Frequency Curves in Biology and Statistics* (Astronomical Laboratory, Noordhoff, Groningen).

Kolmogorov, A. N. [1962] "A refinement of previous hypotheses concerning the local structure of turbulence in viscous incompressible fluid at high raynolds number," *J. Fluid Mech.* **13**, 82–85.

Ladoy, P., Schmitt, F., Schertzer, D. & Lovejoy, S. [1993a] "Variabilité temporelle des observations pluviométriques à nimes," *Comptes Rendues Acad. des Sci.* **317**, 775–782.

Ladoy, P., Schmitt, F., Schertzer, D. & Lovejoy, S. [1993b] "Analyse multifractale de la variabilité temporelle des observations pluviometriques a nîmes," *Comptes Rendus de l'Académie des Sciences de Paris*, in press.

Lamperti, J. [1962] "Semi-stable stochastic processes," *Trans. Amer. Math. Soc.* **104**, 62–78.

Lavallée, D., Lovejoy, S. & Schertzer, D. [1991] "On the determination of the codimension function," *Non-Linear Variability in Geophysics*: *Scaling and Fractals*, eds. Schertzer, D. & Lovejoy, S. (Kluwer), pp. 99–110.

Lazarev, A., Schertzer, D., Lovejoy, S. & Chigirinskaya, Y. [1994] "Unified multifractal atmospheric dynamics tested in the tropics: Part II, vertical scaling and generalized scale invariance," *Nonlin. Process. Geophys.* **1**, 115–123.

Lilley, M., Lovejoy, S., Strawbridge, K. & Schertzer, D. [2004] "23/9 dimensional anisotropic scaling of passive admixtures using lidar data of aerosols," *Phys. Rev. E* **70**, 036307-1-7.

Lopez, R. E. [1979] "The log-normal distribution and cumulus cloud populations," *Mon. Wea. Rev.* **105**, 865–872.

Lorenz, E. N. [1963] "Deterministic nonpereodic flow," *J. Atmos. Sci.* **20**, 130–141.

Lorenz, E. N. [1969] "The predictability of a flow which possesses many scales of motion," *Tellus* **21**, 289–307.

Lovejoy, S. & Schertzer, D. [1998] "Stochastic chaos, symmetry and scale invariance: From art to the weather and back again," *Eco-tec: Architecture of the in-Between*, ed. Marras, A. (Storefront Book series, copublished with Princeton Architectural Press), pp. 80–99.

Lovejoy, S. & Schertzer, D. [2007] "Scale, scaling and multifractals in geophysics twenty years on," *Nonlinear Dynamics in Geosciences*, eds. Tsonis, A. A. & Elsner, J. (Springer, NY).

Lovejoy, S., Tuck, A. F., Hovde, S. J. & Schertzer, D. [2007] "Is isotropic turbulence relevant in the atmosphere?" *Geophys. Res. Lett.* **34**, L14802.

Lovejoy, S., Schertzer, D. & Allaire, V. [2008a] "The remarkable wide range spatial scaling of TRMM precipitation," *J. Atmos. Res.* **90**, 10–32.

Lovejoy, S., Schertzer, D., Lilley, M., Strawbridge, K. & Radkevich, A. [2008b] "Scaling turbulent atmospheric stratification, Part I: Turbulence and waves," *Q. J. Meteorol. Soc.* **134**, 277–300.

Lovejoy & Schertzer [2010] "Towards a new synthesis for atmospheric dynamics: Space–time cascades," *Atmospheric Research* **96**, 1–52.

Lovejoy, S. & Schertzer, D. [2012] *Multifractal Cascades and the Emergence of Atmospheric Dynamics* (Cambridge Univeristy Press, Cambridge, U.K.), in press.

Lévy, P. [1925] *Calcul des Probabilites* (Gautier-Villars, Paris).

Lévy, P. [1937] *Théorie de l'Addition des Variables Aléatoires* (Gauthiers Villars, Paris).

Macor, J., Schertzer, D. & Lovejoy, S. [2007] "Multifractal methods applied to rain forecast using radar data," *La Houille Blanche* **4**, 92–98.

Mandelbrot, B. B. [1974] "Intermittent turbulence in self-similar cascades: Divergence of high moments and dimension of the carrier," *J. Fluid Mech.* **62**, 331–350.

Mandelbrot, B. B. [1977] *Fractals*, *Form*, *Chance and Dimension* (Freeman, San Francisco).

Mandelbrot, B. B. [1983] *The Fractal Geometry of Nature* (Freeman, San Francisco).

Mandelbrot, B. [1985] "Self-affine fractal sets, I: The basic fractal dimensions," *Fractals in Phys.*, eds. Pietronero, L. & Tosatti, E. (North-Holland, Amsterdam), pp. 3–16.

Mandelbrot, B. [1989] "Fractal geometry: What is it and what does it do?" *Fractals in the Natural Sciences*, eds. Fleischman, M., Tildesley, D. J. & Ball, R. C. (Princeton University Press, Princeton), pp. 3–16.

Mandelbrot, B. [1991] "Random multifractals: Negative dimensions and the resulting limitations of the thermodynamic formalism," *Turbulence and Stochastic Processes*, eds. Hunt, J. C. R. *et al.* (The Royal Society, London), pp. 79–88.

Marsan, D., Schertzer, D. & Lovejoy, S. [1996] "Causal space-time multifractal processes: Predictability and forecasting of rain fields," *J. Geophy. Res.* **101**, D21, 26,333–26,346.

McAlsister, D. [1879] "The law of the geometric mean," *Proc. Roy. Soc.* **29**, 367.

Meneveau, C. & Sreenivasan, K. R. [1987] "Simple multifractal cascade model for fully develop turbulence," *Phys. Rev. Lett.* **59**, 1424–1427.

Mesard, M., Parisi, G. & Virascoro, M. A. [1987] *Spin Glass Theory and Beyond* (World Scientific, Singapore).

Metivier, M. [1982] *Semimartingales: A Course on Stochastic Processes* (Walter de Gruyter, Berlin, NY).

Nicolis, C. [1981] "Solar variability and stochastic effect on climate," *Sol. Phys.* **74**, 473–478.

Nicolis, C. [1982] "Stochastic aspects of climatic transitions," *Tellus* **14**, 1–9.

Nicolis, C. & Nicolis, G. [1984] "Is there a climate attractor?" *Nature* **311**, 529–532.

Novikov, E. A. & Stewart, R. [1964] "Intermittency of turbulence and spectrum of fluctuations in energy-disspation," *Izv. Akad. Nauk. SSSR. Ser. Geofiz.* **3**, 408–412.

Obukhov, A. [1962] "Some specific features of atmospheric turbulence," *J. Geophys. Res.* **67**, 3011.

Orszag, S. A. [1970] "Indeterminacy of the moment problem for intermittent turbulence," *Phys. Fluids* **13**, 2211–2212.

Palmer, T. & Williams, P. [2010] *Stochastic Physics and Climate Modelling* (Cambridge University Press, Cambridge, U.K.).

Parisi, G. & Frisch, U. [1985] "On the singularity structure of fully developed turbulence," *Turbulence and Predictability in Geophysical Fluid Dynamics and Climate Dynamics*, eds. Ghil, M. *et al.* (North Holland, Amsterdam), pp. 84–88.

Richardson, L. F. [1922] *Weather Prediction by Numerical Process* (Cambridge University Press republished by Dover, 1965).

Sattinger, D. H. & Weaver, O. L. [1986] *Lie Groups and Algebras with Applications to Physics, Geometry and Mechanics* (Springer-Verlag, NY, Berlin).

Schertzer, D. & Lovejoy, S. [1983] *On the Dimension of Atmospheric Motions* (IUTAM).

Schertzer, D. & Lovejoy, S. [1984] "On the dimension of atmospheric motions," *Turbulence and Chaotic Phenomena in Fluids*, ed. Tatsumi, T. (Elsevier Science Publishers B. V., Amsterdam), pp. 505–512.

Schertzer, D. & Lovejoy, S. [1985a] "Generalised scale invariance in turbulent phenomena," *Physico-Chem. Hydrodyn. J.* **6**, 623–635.

Schertzer, D. & Lovejoy, S. [1985b] "The dimension and intermittency of atmospheric dynamics," *Turbulent Shear Flow 4*, ed. Launder, B. (Springer-Verlag), pp. 7–33.

Schertzer, D. & Lovejoy, S. [1987] "Physical modeling and analysis of rain and clouds by anisotropic scaling multiplicative processes," *J. Geophys. Res.* **8**, 9693–9714.

Schertzer, D. & Lovejoy, S. [1988] "Multifractal simulations and analysis of clouds by multiplicative processes," *Atmosph. Res.* **21**, 337–361.

Schertzer, D., Lovejoy, S., Visvanathan, R., Lavallée, L. & Wilson, J. [1988] "Universal multifractals in turbulence," *Fractal Aspects of Materials: Disodered Systems*, eds. Weitz, D. A., Sander, L. M. & Mandelbrot, B. B. (MRS, Pittsburgh), pp. 267–270.

Schertzer, D. & Lovejoy, S. [1989a] "Generalized scale invariance and multiplicative processes in the atmosphere," *Pure Appl. Geophys.* **130**, 57–81.

Schertzer, D. & Lovejoy, S. [1989b] "Nonlinear variability in geophysics: Multifractal analysis and simulation," *Fractals: Physical Origin and Consequences*, ed. Pietronero, L. (Plenum, NY), pp. 49.

Schertzer, D. & Lovejoy, S. [1991] "Nonlinear geodynamical variability: Multiple singularities, universality and observables," *Non-Linear Variability in Geophysics: Scaling and Fractals*, eds. Schertzer, D. & Lovejoy, S. (Kluwer), pp. 41–82.

Schertzer, D. & Lovejoy, S. [1992] "Hard and soft multifractal processes," *Physica A* **185**, 187–194.

Schertzer, D. & Lovejoy, S. [1993] Lecture Notes: Nonlinear Variability in Geophysics 3: Scaling and Mulitfractal Processes in Geophysics (Institut d'Etudes Scientifique de Cargèse, Cargèse, France).

Schertzer, D., Lovejoy, S. & Lavallée, D. [1993] "Generic multifractal phase transitions and self-organized criticality," *Cellular Automata: Prospects in Astronomy and Astrophysics*, eds. Perdang, J. M. & Lejeune, A. (World Scientific), pp. 216–227.

Schertzer, D. & Lovejoy, S. [1994] "Mulitfractal generation of self-organized criticality," *Fractals in the Natural and Applied Sciences*, ed. Novak, M. M. (North-Holland, Amsterdam), pp. 325–340.

Schertzer, D. & Lovejoy, S. [1997] "Universal multifractals do exist!" *J. Appl. Meteor.* **36**, 1296–1303.

Schertzer, D., Lovejoy, S., Schmitt, F., Tchiguirinskaia, I. & Marsan, D. [1997] "Multifractal cascade dynamics and turbulent intermittency," *Fractals* **5**, 427–471.

Schertzer, D., Larcheveque, M., Duan, J. & Lovejoy, S. [1999] "Genaralized stable multivariate distribution and anisotropic dilations," IMA Preprint (IMA, U. od Minnesota, Minneapolis).

Schertzer, D., Lovejoy, S. & Hubert, P. [2002] "An introduction to stochastic multifractal fields," *Isfma Symp. Environmental Science and Engineering with Related Mathematical Problems*, eds. Ern, A. & Liu, W. (High Education Press, Beijing), pp. 106–179.

Schertzer, D. & Lovejoy, S. [2004a] "Space-time complexity and multifractal predictability," *Physica A* **338**, 173–186.

Schertzer, D. & Lovejoy, S. [2004b] "Uncertainty and predictability in geophysics: Chaos and multifractal insights," *State of the Planet, Frontiers and Challenges in Geophysics*, eds. Sparks, R. S. J. & Hawkesworth, C. J. (AGU, Washington), pp. 317–334.

Schertzer, D., Tchiguirinskaia, I., Lovejoy, S. & Hubert, P. [2010] "No monsters, no miracles: In nonlinear sciences hydrology is not an outlier!" *Hydrol. Sci. J.* **55**, 965–979.

Schertzer, D., Tchiguirinskaia, I., Lovejoy, S. & Tuck, A. F. [2012] "Quasi-geostrophic turbulence and generalized scale invariance, a theoretical reply," *Atmos. Chem. Phys.* **12**, 327–336.

Schmitt, F., Schertzer, D., Lovejoy, S. & Brunet, Y. [1994] "Empirical study of multifractal phase transitions in atmospheric turbulence," *Nonlin. Process. Geophys.* **1**, 95–104.

Schoenberg, I. J. [1938] "Metric spaces and completely monotone functions," *Ann. Math.* **39**, 811–841.

Schuster, H. G. [1988] *Deterministic Chaos* (VCH, NY).

Sedov, L. [1972] *Similitudes et Dimensions en Mécanique* (MIR, Moscow).

Sonin, A. A. [2004] "A generalization of p-theorem and dimensional analysis," *Proc. Nat. Acad. Sci.*

Speziale, C. G. [1985] "Galilean invariance of subgrid scale stress models in the large-eddy simulation of turbulence," *J. Fluid Mech.* **156**, 55–62.

Stolle, J., Lovejoy, S. & Schertzer, D. [2009] "The stochastic cascade structure of deterministic numerical models of the atmosphere," *Nonlin. Process. Geophys.* **16**, 607–621.

Szépfalusy, P., Tél, T., Csordas, A. & Kovas, Z. [1987] "Phase transitions associated with dynamical properties of chaotic systems," *Phys. Rev. A* **36**, 3525.

Tel, T. [1988] "Fractals and multifractals," *Zeit. Naturforsch* **43a**, 1154–1174.

Weyl, H. [1952] *Symmetry* (Princeton University Press, Princeton, NJ).

Wilson, J. [1991] *Physically Based Stochastic Modelling of Rain and Cloudfields* (McGill University).

Wilson, K. G. & Kogut, J. [1974] "The renormalization group and the e expansion," *Phys. Rep.* **12C**, 77–200.

Yaglom, A. M. [1966] "The influence on the fluctuation in energy dissipation on the shape of turbulent characteristics in the inertial interval," *Sov. Phys. Dokl.* **2**, 26–30.

Zee, A. [1986] *Fearful Symmetry*: *The Search for Beauty in Modern Physics* (Colliers Books, MacMillan Publishing Company, NY).